Electronic Supporting Information

Efficient Light Harvesting in Self-assembled Organic Luminescent Nanotubes

Shubhra K. Bhaumik,[a] Dibyendu Maity,[b] Ipsita Basu,[b] Suman Chakrabarty*[b] and Supratim Banerjee*[a]

[a] Shubhra. K. Bhaumik, and Supratim Banerjee- Department of Chemical Sciences, Indian Institute of Science Education and Research Kolkata, Mohanpur, West Bengal, India
[b] Dibyendu Maity, Ipsita Basu, and Suman Chakrabarty- Department of Chemical and Biological Sciences, S. N. Bose National Centre for Basic Sciences, Kolkata, India

Email: supratim.banerjee@iiserkol.ac.in; sumanc@bose.res.in

Table of Contents

Experimental Procedures

1. Materials and Method:

All reagents were purchased from commercially available sources and used without further purification. 4-(pyridin-4-yl)benzaldehyde, (4-(cyanomethyl)phenyl)boronic acid and 4-bromopyridine hydrochloride were purchased from Combi-Blocks. Nile Red, Nile Blue perchlorate, tris(hydroxymethyl)aminomethane, tetrabutylammonium hydroxide 30-hydrate, 1-bromooctane, 1-bromodecane, 1-bromododecane, and tert-butanol were purchased from Sigma-Aldrich. 1-bromohexane was purchased from Spectrochem Pvt. Ltd. Heparin sodium salt from hog intestine was purchased from TCI chemicals. UV-Vis spectroscopic measurements were carried out in Agilent Technologies Cary 8454 spectrophotometer. Emission spectroscopic measurements were carried out in Horiba Fluoromax 4 spectrofluorometer. Absolute quantum yields were measure using Quanta-phi integrating sphere fitted with a Horiba Fluoromax 4 spectrofluorometer. Fluorescence images were taken under 365 nm UV lamp. A Horiba Jobin Yvon Fluorocube instrument fitted with a 340 nm diode laser excitation source (with a temporal resolution of 70 ps) was used for the time-resolved fluorescence experiments applying the time correlated single photon counting (TCSPC) method. Steady-state fluorescence anisotropy measurements were carried out in Hitachi-7000 spectrofluorometer. TEM images were recorded in a JEOL JEM2100 PLUS instrument.

Computational Details: All-atom molecular dynamics (MD) simulations have been performed using the GROMACS[S1] (version 2019.5) software package. TIP3P[S2] model has been chosen to represent water in our simulations. Force field parameters of the dye molecules (**12CS12** and Nile Red) and heparin have been obtained from the CHARMM36[S3] force field and CGENFF[S4, S5] (version 4.6) web server.

We have simulated three systems: (i) 100 **12CS12** dye molecules dispersed in water, (ii) 1 Heparin and 100 **12CS12** dye molecules dispersed in water, and (iii) 1 Heparin, 100 **12CS12** and 3 Nile Red dye molecules dispersed in water. In the cubic simulation box of dimension 14.26 nm, we have inserted 100 **12CS12** molecules randomly and solvated with nearly 92000 water molecules, which yields an effective concentration of ~587mM. We have used significantly higher concentrations as compared to the experiments in order to achieve rapid and extended aggregate formation within the simulation timescale (~500ns).

We have used the leap-frog integrator to integrate Newton's equations of motion with a time step of 2 fs. The LINCS[S6] algorithm has been applied to constrain the bond lengths. The Van der Waals' and short-range nonbonded electrostatics interactions had a cutoff radius of 1.0 nm. Long-range electrostatic interactions were calculated using the Particle Mesh Ewald (PME)[S7] method. Periodic boundary conditions (PBC) were applied in all 3 directions. The temperature was maintained at 300 K using the velocity rescale[S8] method with a relaxation time of 1 ps, and the pressure was kept constant at 1 atm using the Parinello-Rahman[S9] barostat. At first, all the systems were energy minimized using the Steepest Descent algorithm. Then, the energy-minimized structures were subjected to NVT equilibration of 100 ps at 300K. After that, equilibrium configurations were put into the NPT ensemble at 300K, 1 bar for 1ns. Finally, the aggregation process for each system has been monitored in the production run under the NPT ensemble for up to 500 ns.

2. Synthetic Procedures:

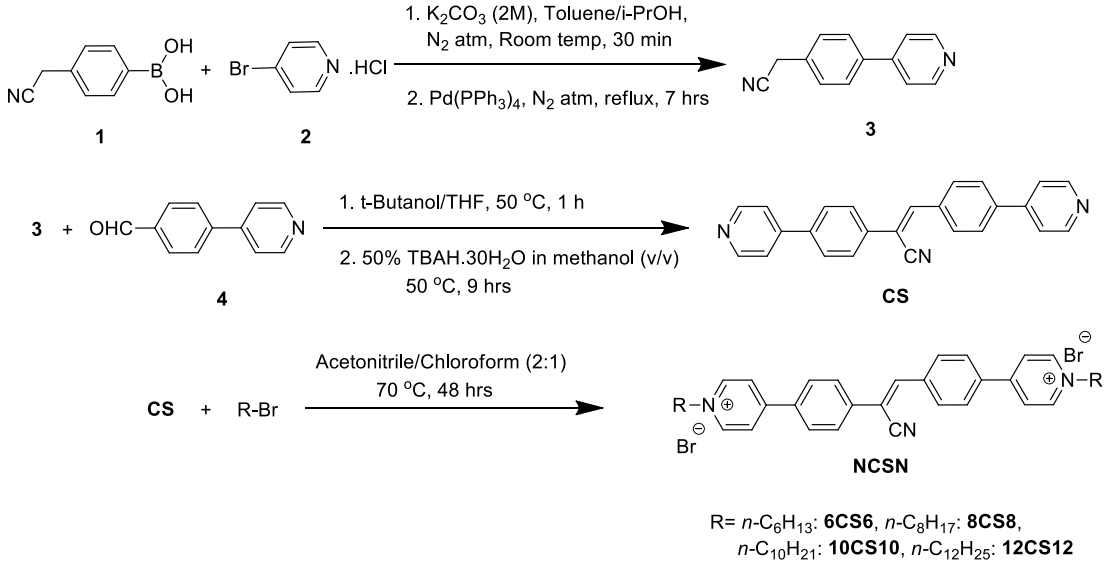

Scheme S1. Synthetic route for the preparation of **NCSN**s

Preparation of **NCSN** derivatives are described in our previous reports.[S10,S11]

3. Preparation of Solutions:

Preparation of solution of NCSNs:

Initially, stock solutions of **NCSN**s (N = 6, 8, 10, 12) were prepared by dissolving the solid powders in spectroscopic grade dimethyl sulfoxide (DMSO). The DMSO solutions were then diluted by 5 mM tris-HCl buffer made in Milli-Q water to get desired solutions having 1% DMSO as the final DMSO fraction. Solution of **6CS6** in aqueous buffer was equilibrated for 10 min whereas solutions of **SP8**, **SP10** and **SP12** in aqueous buffer were equilibrated for 1 hr.

Preparation of heparin solution:

The disaccharide unit shown in Chart S1a is taken as the repeat unit of heparin for the molecular weight calculation. Though the supplied heparin contains only 30-40% materials with the active sequence of repeat units, the whole sample can still bind through the anionic polysaccharide unit irrespective of whether the repeat units are in active sequence or not. The molecular weight of the repeat unit is 665.40 g/mole. Heparin stock solutions were prepared in buffer and further diluted during titration.

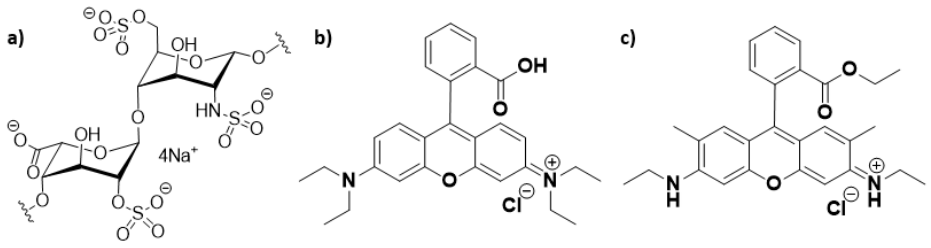

Chart S1. a) A common repeat unit of heparin chain. Chemical structures of b) Rhodamine B and c) Rhodamine 6G

4. Titration Procedures:

At first, heparin solution was added to freshly prepared and equilibrated **SP** solutions in aqueous buffer and further equilibrated for 10-15 min. Then the acceptor (Rhodamine B/Rhodamine 6G/Nile Red/Nile Blue) dyes were added to it and data were recorded in a spectrofluorometer after 5 min.

5. Quantum Yield Calculation Method:

Absolute quantum yield measurement of aggregated solutions:

Absolute quantum yields of **6CS6** (5 µM), **SP8** (10 µM), **SP10** (5 µM), **SP12** (5 µM) without and with heparin (10 µM) in aqueous buffer were measured using an integrating sphere.

6. Energy Transfer Efficiency Calculation

Energy transfer (ET) efficiency is the percentage of the absorbed energy that is transferred to the acceptor and is expressed by the following equation

$$ET = (1 - I/I_0) \times 100\%$$

where, I and I_0 are the fluorescence intensities without and in presence of acceptor in aqueous buffer.

7. Antenna Effect Calculation

The antenna effect (AE) value under certain concentrations of donor and acceptor is the ratio of the emission intensities at the emission maximum of the acceptor in presence of the donor upon excitation of the donor and is expressed as follows-

$$AE = \frac{I_{\text{Em max. of A}}^{\text{D+A } (\lambda_{ex} = 365 \text{ nm})} - I_{\text{Em max. of A}}^{\text{D } (\lambda_{ex} = 365 \text{ nm})}}{I_{\text{Em max. of A}}^{\text{A } (\lambda_{ex} = \text{abs maxima of A})}}$$

$I_{\text{Em max. of A}}^{\text{D+A } (\lambda_{ex} = 365 \text{ nm})}$ = Emission intensity of acceptor in the presence of donor upon the excitation of donor

$I_{\text{Em max. of A}}^{\text{D } (\lambda_{ex} = 365 \text{ nm})}$ = Emission intensity of donor (at acceptor maximum emission wavelength) in the absence of acceptor upon the excitation of donor

$I_{\text{Em max. of A}}^{\text{A } (\lambda_{ex} = \text{abs maxima of A})}$ = Emission intensity of acceptor in the presence of donor upon the excitation of acceptor

Results and Discussion

1. Photophysical Properties of SPs and HSPs in Aqueous Buffer:

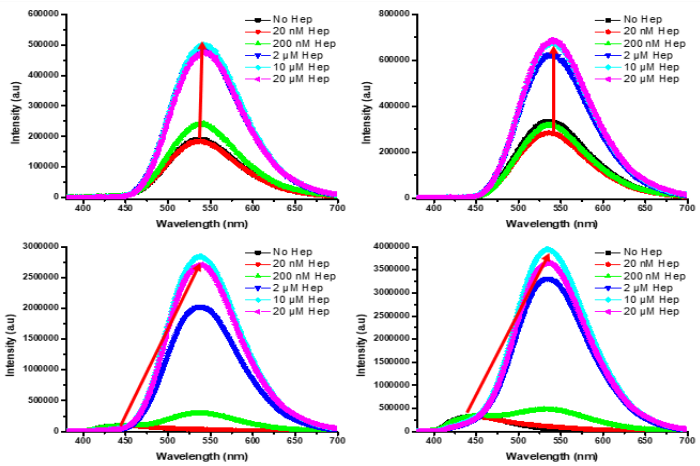

Fig. S1 Emission spectra of (a) **SP10** (**10CS10**:5 µM), (b) **SP12** (**12CS12**:5 µM) (c) **SP8** (**8CS8**:5 µM), and (d) **6CS6** and their co-assemblies with heparin (10 µM) in aqueous buffer.

Table S1. DLS data for the average size and zeta potential (ζ) of the self-assembled **CS** derivatives before and after heparin addition in aqueous buffer (5 mM tris-HCl, 99:1 water/DMSO, pH 7.4).

CS derivatives	Size w/o- heparin (nm)	Size w/- heparin (nm)	ζ w/o- heparin (mV)	ζ w/- heparin (mV)
8CS8 (10 µM)	170.1 (KCPS=295)	952 (KCPS=152)	0.508	-24
10CS10 (5 µM)	288 (KCPS=179)	1636 (KCPS=164)	27.3	-29.4
12CS12 (5 µM)	208 (KCPS=384)	1186 (KCPS=206)	27	-31

Table S2. Absolute quantum yields (Φ) and average lifetimes (τ_{avg}) of **CS** derivatives without and with heparin in aqueous buffer (5 mM tris-HCl, 99:1 water/DMSO, pH 7.4).

CS derivative	λ_{abs} and λ_{em} w/o-heparin	Stokes shift w/o-heparin	Φ (%) w/o-heparin	λ_{abs} and λ_{em} w/-heparin	Stokes shift w/-heparin	Φ (%) w/-heparin	τ_{avg} (ns) w/o-heparin	τ_{avg} (ns) w/-heparin
6CS6 (5 µM)	λ_{abs}=361 nm λ_{em}=453 nm	92 nm	0.66	λ_{abs}=366 nm λ_{em}=536 nm	170 nm	56.70	0.45 (453 nm)	22.06 (536 nm)
8CS8 (10 µM)	λ_{abs}=361 nm λ_{em}=453 nm, 538 nm	92 nm, 177 nm	0.85	λ_{abs}=366 nm λ_{em}=540 nm	174 nm	24.26	0.19 (453 nm), 2.49 (540 nm)	19.74 (538 nm)
10CS10 (5 µM)	λ_{abs}=359 nm λ_{em}=540 nm	181 nm	7.87	λ_{abs}=361 nm λ_{em}=540 nm	179 nm	24.8	4.3 (540 nm)	17.36 (540 nm)
12CS12 (5 µM)	λ_{abs}=358 nm λ_{em}=540 nm	182 nm	10.52	λ_{abs}=361 nm λ_{em}=540 nm	179 nm	22.36	6.97 (540 nm)	9.98 (540 nm)

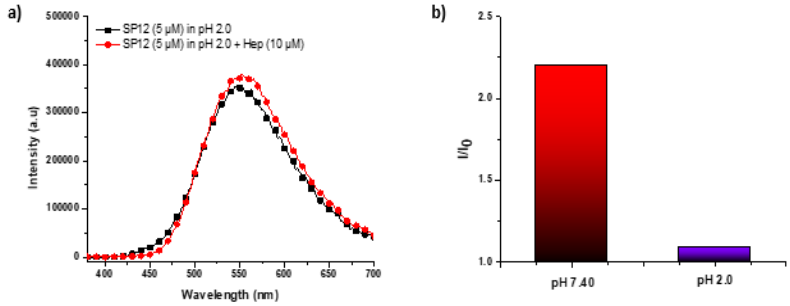

Fig. S2 (a) Emission spectra of **SP12** (**12CS12**:5 µM) in aqueous buffer containing HCl (pH 2.0) without and with heparin (10 µM). (b) A bar diagram comparing the I/I_0 value of **SP12** in the presence of heparin at aqueous buffer (pH 7.40) and at buffer containing HCl (pH 2.0).

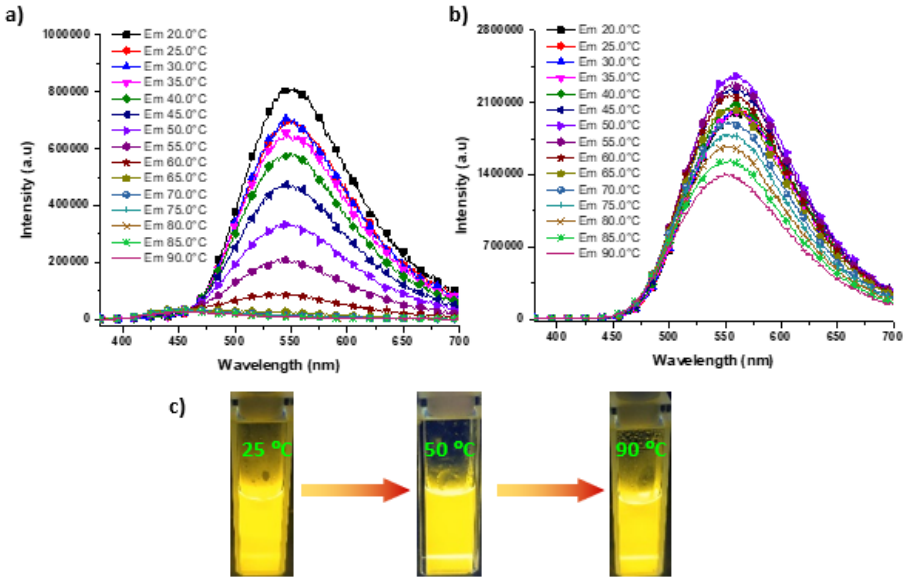

Fig. S3 (a) Emission spectra of (a) **SP12** (**12CS12**:5 μM) and (b) **HSP12** (**12CS12**:5 μM; Heparin: 10 μM) in aqueous buffer (pH 7.40) at different temperatures. (c) Fluorescent images of **HSP12** (**12CS12**:5 μM; Heparin: 10 μM) in aqueous buffer (pH 7.40) at different temperatures.

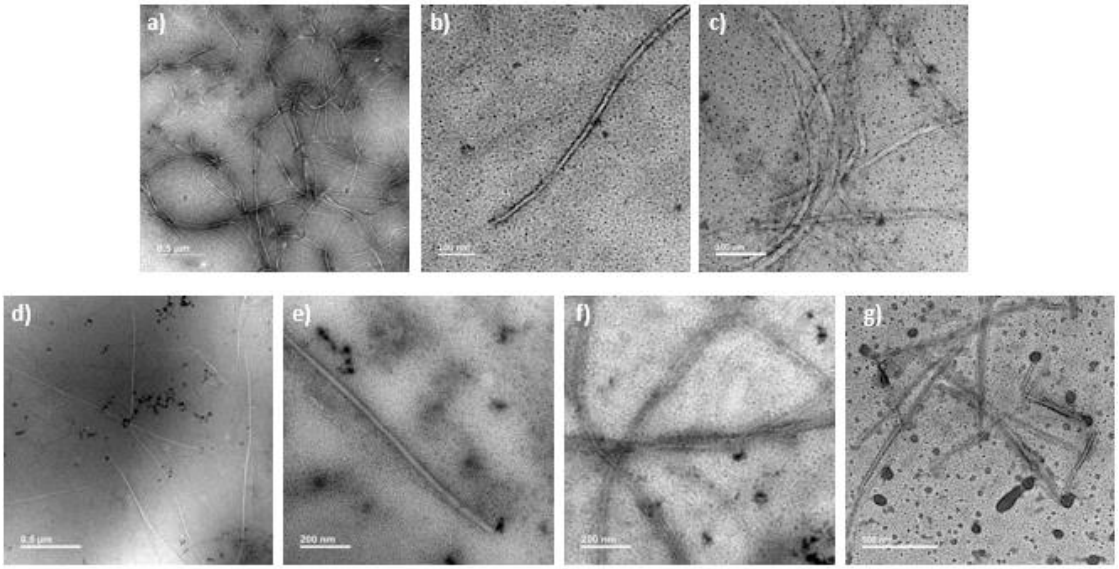

Fig. S4 Transmission Electron Microscopic (TEM) images of dried solutions of (a, b) **HSP12** [**12CS12**: 5 μM, heparin: 10 μM], c) **HSP12** [**12CS12**: 5 μM, heparin: 10 μM]-Nile Red (**NR**) (50 nM) and (d-f) **HSP10** [**10CS10**: 5 μM, heparin: 10 μM]. (f) TEM image of **HSP12** [**12CS12**: 5 μM, heparin: 1 μM]. A 0.01% uranyl acetate solution was used as staining agent.

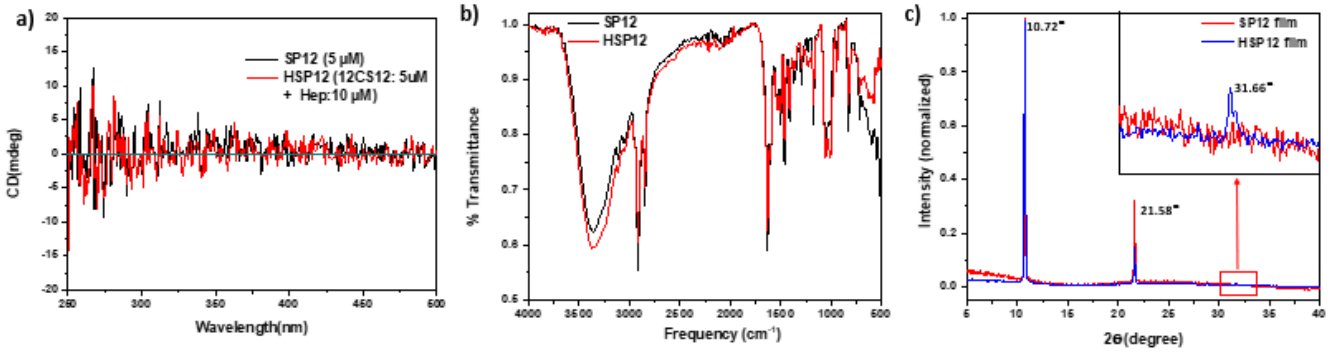

Fig. S5 (a) CD spectra of **SP12** (5 μM) and **HSP12** [**12CS12**: 5 μM), heparin: 10 μM) in aqueous buffer (99:1 water-DMSO, 5 mM tris-HCl, pH 7.4). (b) FT-IT spectra and (d) PXRD data of SP12 and HSP12 obtained after drying from aqueous buffer (99:1 water-DMSO, 5 mM tris-HCl, pH 7.4).

Determination of shape of the self-assembly and co-assembly by MD simulation: Asphericity (*b*) and acylindricity (*c*) that can be derived from the eigenvalues of gyration tensor as follows.

$$b = \lambda_z^2 - \frac{1}{2}(\lambda_x^2 + \lambda_y^2)$$
$$c = \lambda_y^2 - \lambda_z^2$$

where λ_z^2, λ_x^2 and λ_y^2 are the principal moments of the gyration tensor and $\lambda_x^2 \leq \lambda_y^2 \leq \lambda_z^2$.

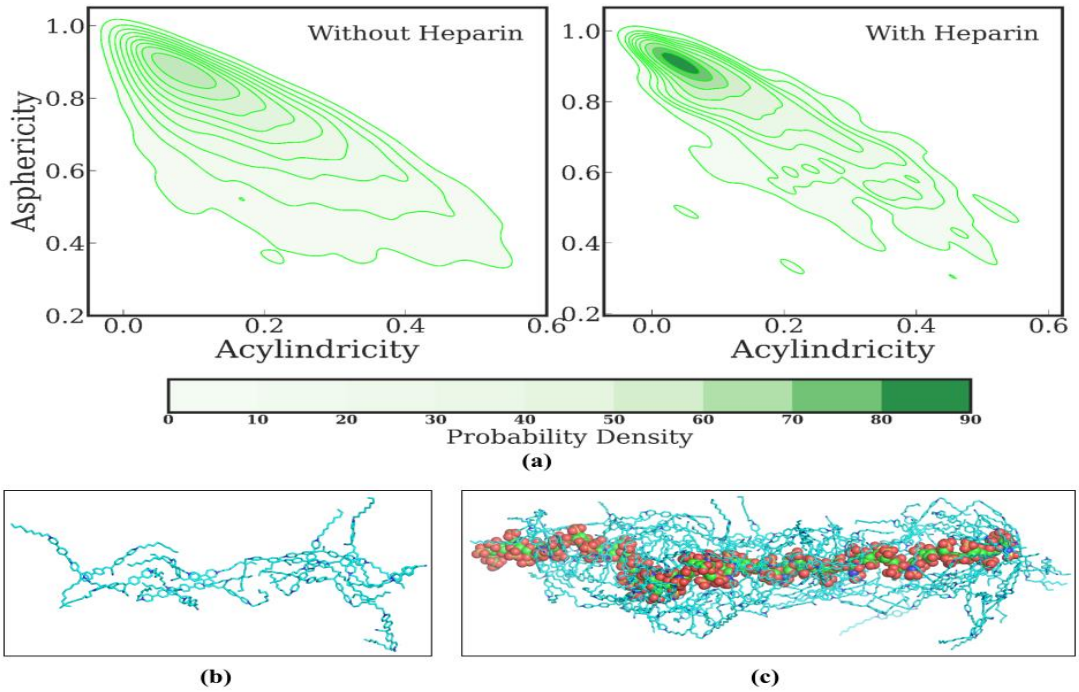

Fig. S6 (a) Joint probability distribution of acylindricity and asphericity of the clusters present in the systems without heparin (left) and with heparin (right). Representative snapshots of the largest clusters are shown in the bottom panels for (b) without heparin and (c) with heparin.

The asphericity (*b*) has a range of zero to one, of which zero refers to the spherically symmetric distribution and one means completely non-spherical, whereas in the case of acylindricity, the value near zero represents perfectly cylindrical distribution and value of one corresponds to the other way. Acylindricity has also the same limit as asphericity. From Fig. 2 it can be concluded that for both the systems (with and without heparin) we have predominantly cylindrical symmetry in the clusters formed. The clusters in the presence of heparin show a sharp maximum in the joint probability density plot near b = 1, and c= 0 indicating the formation of a cylindrical nanotube formed of CS12 dyes wrapped around the heparin polymer.

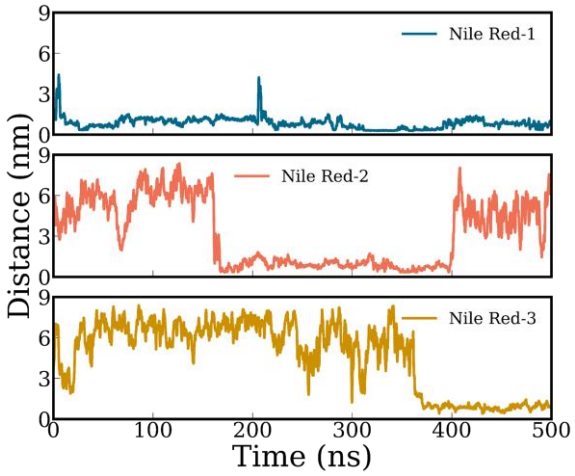

Fig. S7 Time evolution of the minimum distance between the three Nile Red molecules with the heparin strand.

2. Energy Transfer Studies of SPs in Aqueous Buffer:

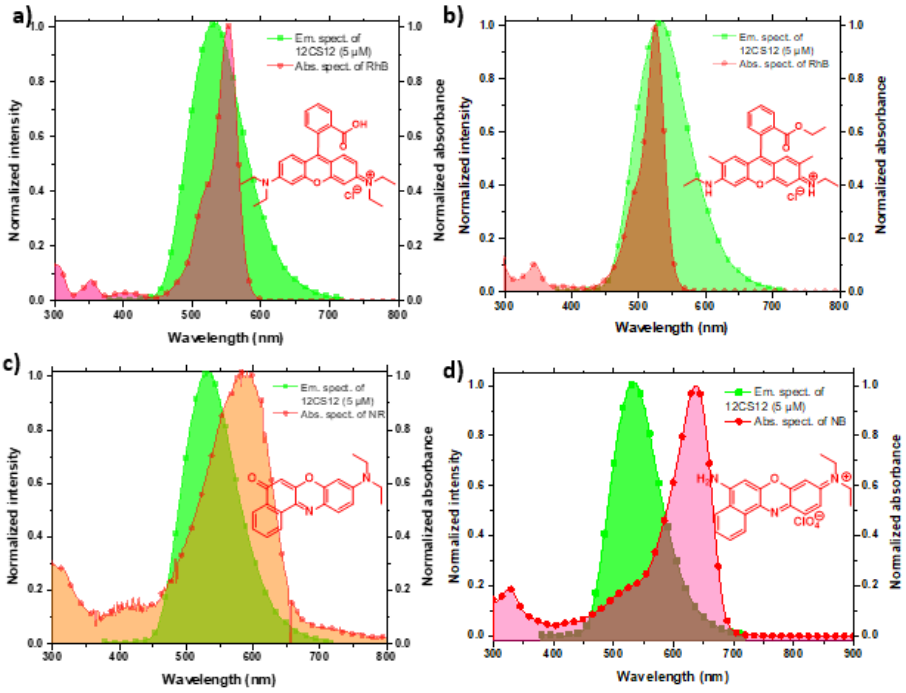

Fig. S8 Spectral overlap of emission of **SP12** (**12CS12:** 5 μM, **B**) and absorption of (a) Rhodamine B (**RhB**), (b) Rhodamine 6G (**Rh6G**), (c) Nile Red (**NR**) and Nile Blue (**NB**) in aqueous buffer (5 mM tris-HCl, 99:1 water/DMSO, pH 7.40).

A. Spectral overlap between SP12 and acceptor dyes:

The overlap integral [$J(\varepsilon)$] values of the emission spectra **SP12** (**12CS12:** 5 μM, **B**) and the absorption spectra of the acceptor dyes were calculated by FluorTools software.

Table S3. Overlap integral [$J(\varepsilon)$] of the emission spectra of **SP12** (**12CS12:** 5 μM, **B**) and the absorption spectra of the acceptor dyes

Rhodamine B (RhB)	Rhodamine 6G (Rh6G)	Nile Red (NR)	Nile Blue (NB)
7.37×10^{-13} $M^{-1}cm^3$	1.26×10^{-13} $M^{-1}cm^3$	7.55×10^{-14} $M^{-1}cm^3$	3.15×10^{-13} $M^{-1}cm^3$

B. Calculation of the radiative rate constant (k_r) of SP12 (12CS12: 5 μM, B):

Radiative rate constant (k_r) of donor [**12CS12** (5 μM)] is calculated using following equation: $k_r = Q_D/\tau$

where, Q_D = Quantum efficiency of donor = 0.105 for **SP12** (**12CS12:** 5 μM)

τ = Average lifetime of the donor in **SP12** (**12CS12:** 5 μM) = 6.97 ns

The radiative rate constant (k_r) of **SP12** (**12CS12:** 5 μM) is determined to be 1.51×10^7 s^{-1}

C. Förster radius (R_0) calculation for SP12-NR:

For any FRET system, Förster Radius (R_0) is calculated by using the following equation-

$$R_0 = 9.78 \times 10^3 \times [k^2 \times n^{-4} \times Q_D \times J(\varepsilon)]^{1/6} \text{ in Å}$$

where, k^2 = Relative orientation in space of the transition dipoles of donor and acceptors which is usually assumed to be 2/3.

n = refractive index of the medium = 1.33 for aqueous buffer

Q_D = Quantum efficiency of donor = 0.105 for **SP12** (**12CS12:** 5 μM) in aqueous buffer

$J(\varepsilon)$ = Overlap integral of emission spectra of donor **SP12** (**12CS12:** 5 μM) and absorption spectra of acceptor [Nile Red (**NR**)] = 7.55×10^{-14} $M^{-1}cm^3$

R_0 for **SP12** (**12CS12:** 5 μM)-**NR** was calculated to be 33.8 Å (~3.4 nm).

D. Energy transfer studies from SPs to Nile Red (NR) and Nile Blue (NB):

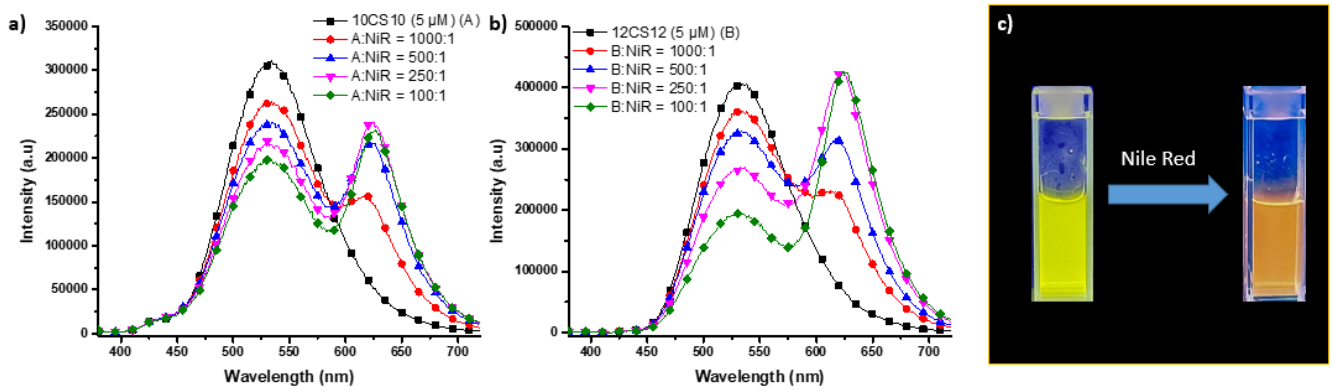

Fig. S9 (a) Emission spectral changes of **SP10** (**10CS10:** 5 μM, **A**) and (b) **SP12** (**12CS12:** 5 μM, **B**) with increasing concentration of Nile Red (**NR**) in aqueous buffer. (b) Image of **SP12** (**12CS12**: 5 μM) without and with **NR** (D:A = 250:1) under UV 365 nm.

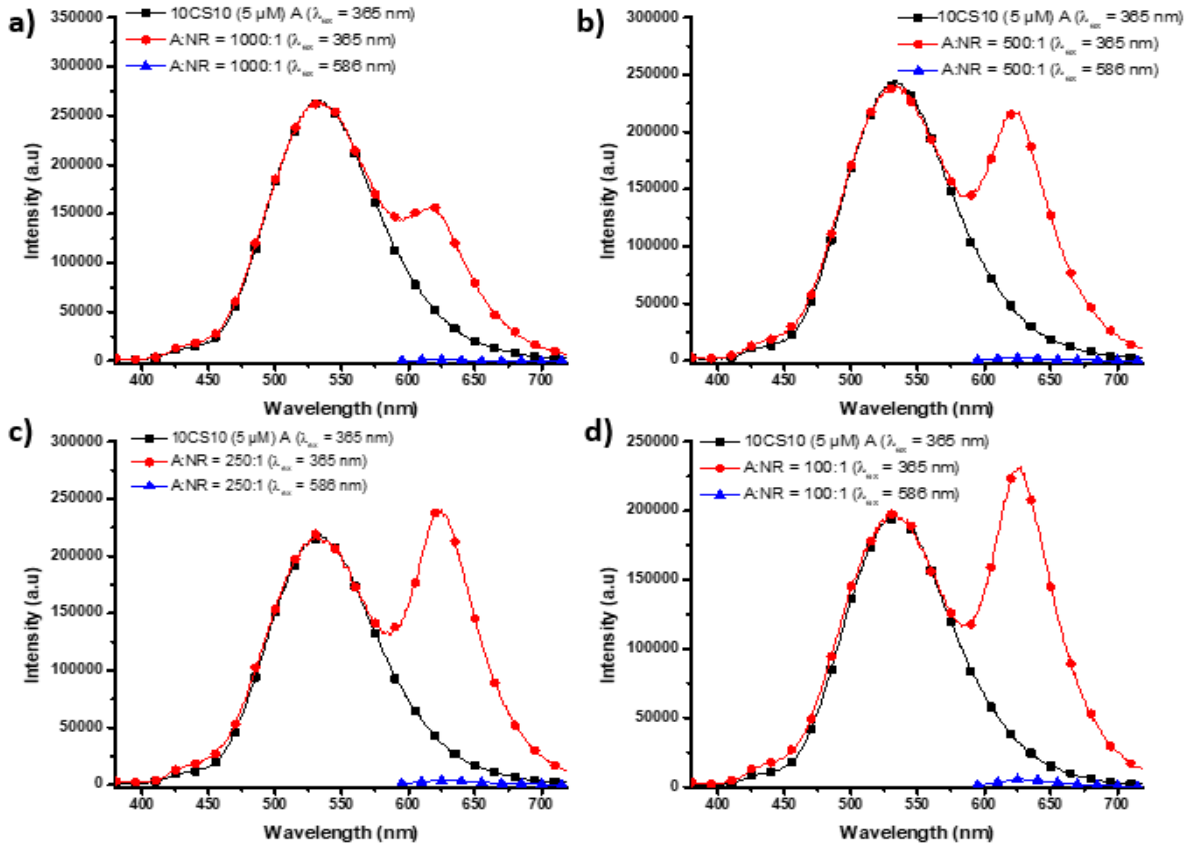

Fig. S10 Emission spectra of **SP10 (10CS10**: 5 μM, **A**) and in the presence of **NR** in aqueous buffer at (a) 1000:1, (b) 500:1, (c) 250:1 and (d) 100:1 donor/acceptor ratios. Red trace: donor emission (λ_{ex} = 365 nm) and blue trace: acceptor emission (λ_{ex} = 586 nm). Black trace represents emission spectrum of **SP10** (**10CS10:** 5 μM, **A**) (λ_{ex} = 365 nm) which was normalized to the intensity at 540 nm of the red trace.

Table S4. ET efficiency (%) and Antenna effect (AE) values in **SP10**-**NR** (**10CS10**: 5 μM) at different donor/acceptor ratios.

Donor/acceptor ratio	ET efficiency	AE
1000:1	15.1%	92
500:1	22.1%	79
250:1	30.5%	55
100:1	36.7%	38

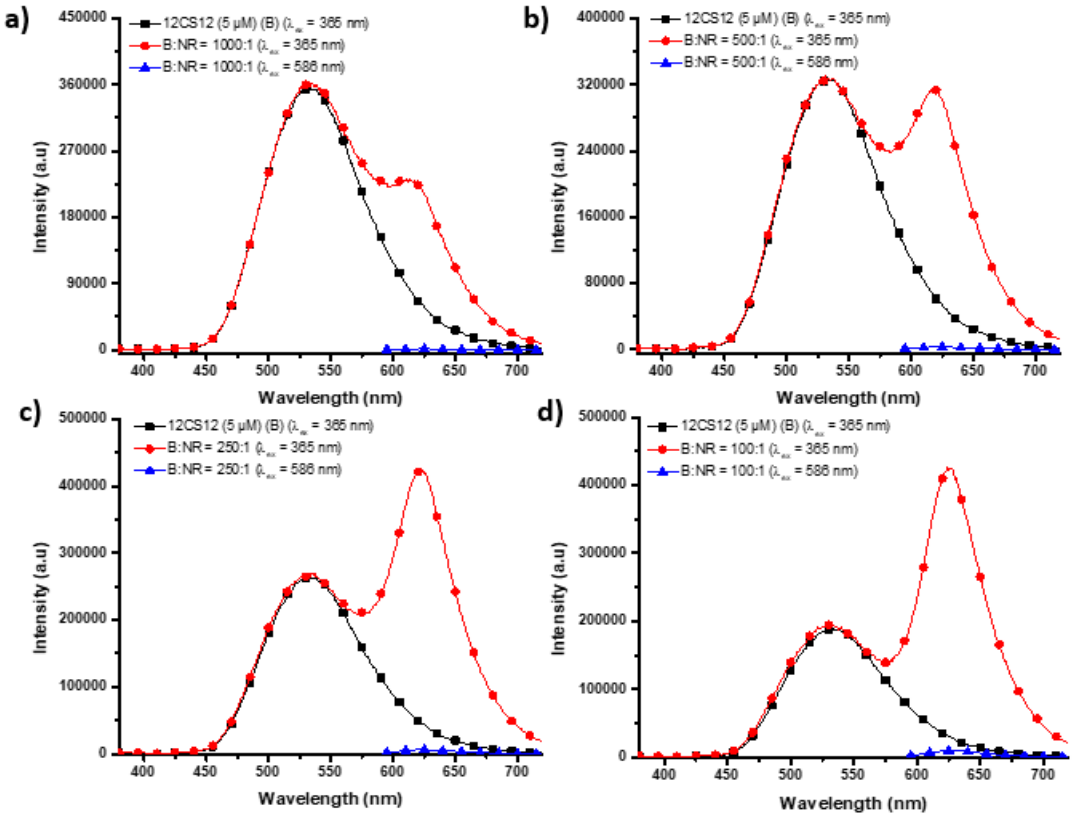

Fig. S11 Emission spectra of **SP12 (12CS12**: 5 μM, **B**) and in the presence of **NR** in aqueous buffer at (a) 1000:1, (b) 500:1, (c) 250:1 and (d) 100:1 donor/acceptor ratios. Red trace: donor emission (λ_{ex} = 365 nm) and blue trace: acceptor emission (λ_{ex} = 586 nm). Black trace represents emission spectrum of **SP12** (**12CS12:** 5 μM, **B**) (λ_{ex} = 365 nm) which was normalized to the intensity at 540 nm of the red trace.

Table S5. ET efficiency (%) and Antenna effect (AE) values in **SP12-NR** (**12CS12**: 5 μM) at different donor/acceptor ratios.

Donor/acceptor ratio	ET efficiency	AE
1000:1	11.0%	138
500:1	19.4%	95
250:1	34.6%	64
100:1	52.4%	41

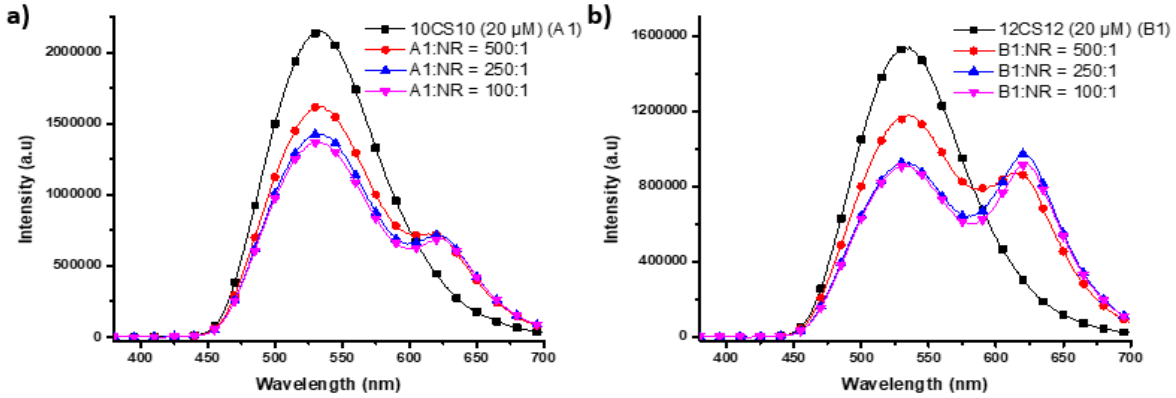

Fig. S12 Emission spectral changes of (a) **SP10 (10CS10**: 20 μM, **A1**) and (b) **SP12 (12CS12**: 20 μM, **B1**) upon increasing concentration of Nile Red (**NR**) in aqueous buffer.

Table S6. ET efficiency (%) and Antenna effect (AE) values in **SP10-NR** (**10CS10**, 20 µM) at different donor/acceptor ratios.

Donor/acceptor ratio	ET efficiency	AE
500:1	23.3%	65.3
250:1	40.6%	50.3
100:1	41.1%	36.8

Table S7. ET efficiency (%) and Antenna effect (AE) values in **SP12-NR** (**12CS12**: 20 µM) at different donor/acceptor ratios.

Donor/acceptor ratio	ET efficiency	AE
500:1	24.7%	57
250:1	33.8%	32
100:1	36.5%	31

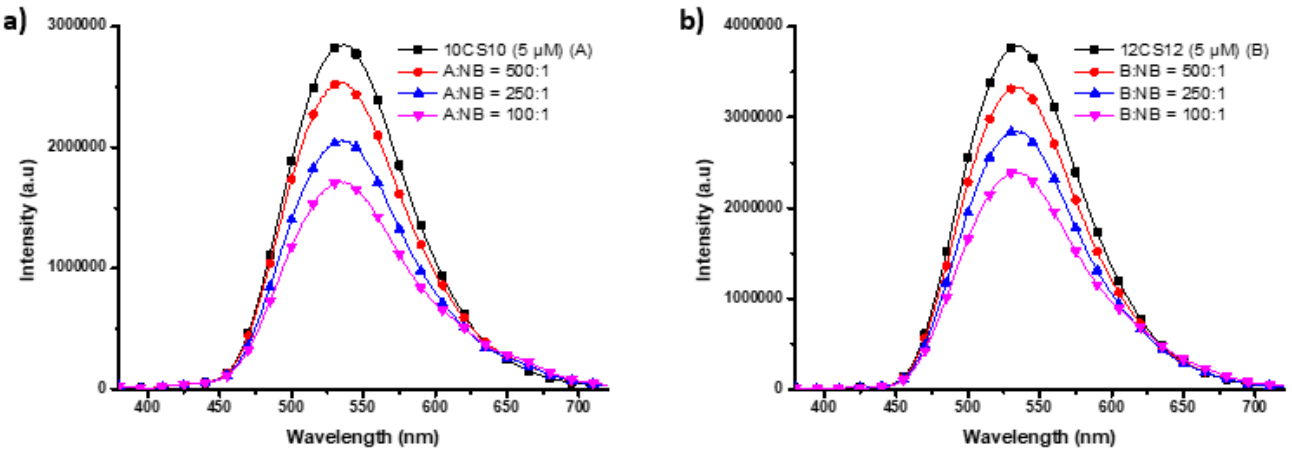

Fig. S13 Emission spectral changes of (a) **SP10** (**10CS10:** 5 µM, **A**) and (b) **SP12** (**12CS12:** 5 µM, **B**) upon increasing concentration of Nile Blue (**NB**) in aqueous buffer.

Table S8. ET efficiency (%) and Antenna effect (AE) values in **SP10-NB** (**10CS10**: 5 µM) at different donor/acceptor ratios.

Donor/acceptor ratio	ET efficiency	AE
500:1	12%	33
250:1	28%	26
100:1	40%	19

Table S9. ET efficiency (%) and Antenna effect (AE) values in **SP12-NB** (**12CS12**: 5 µM) at different donor/acceptor ratios.

Donor/acceptor ratio	ET efficiency	AE
500:1	12%	19
250:1	25%	18
100:1	37%	15

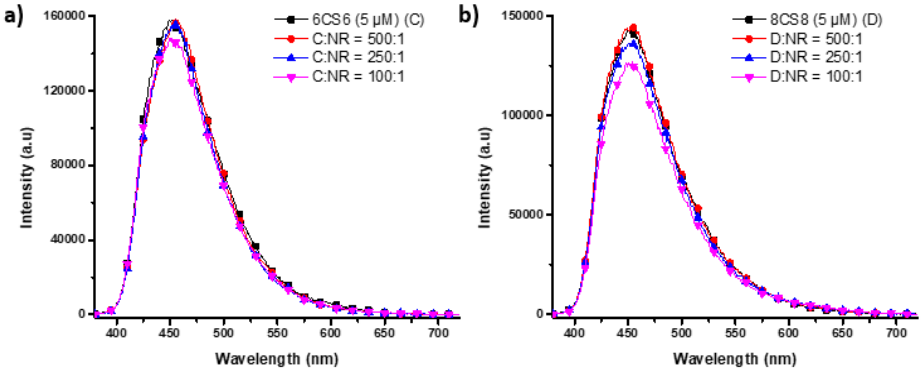

Fig. S14 Emission spectral changes of (a) **6CS6** (5 μM) (**C**) and (b) **SP8 (8CS8**: 5 μM) (**D**) upon increasing concentration of Nile Red (**NR**) in aqueous buffer.

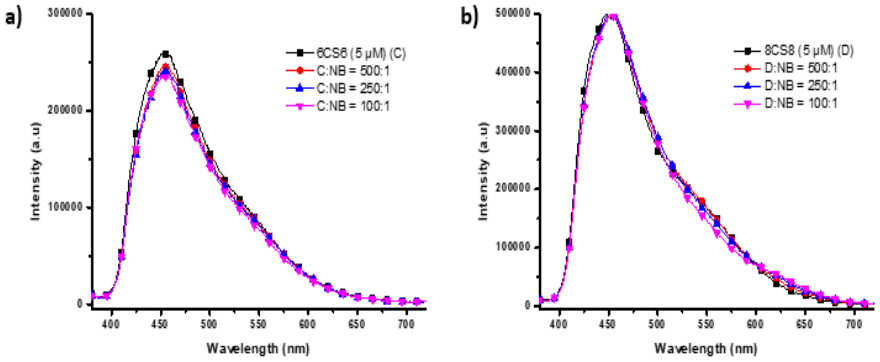

Fig. S15 Emission spectral changes of (a) **6CS6** (5 μM) (**C**) and (b) **SP8 (8CS8**: 5 μM) (**D**) upon increasing concentration of Nile Blue (**NB**) in aqueous buffer.

Table S10. ET efficiency (%) of (a) **6CS6** (5 μM) (**C**) and **SP8 (8CS8**: 5 μM) (**D**) to Nile Red (**NR**) and Nile Blue (**NB**)

Donor/acceptor ratio	**NR**		**NB**	
	6CS6 (5 μM)	**8CS8 (5 μM)**	**6CS6 (5 μM)**	**8CS8 (5 μM)**
100:1	7%	12.5%	9%	13%

Table S11. Steady-state fluorescence anisotropy (r) values of **NR** (50 nM) (λ_{ex} = 586 nm) and **NB** (50 nM) (λ_{ex} = 635 nm) in the presence of **SP10 (10CS10**: 5 μM) and **SP12 (12CS12**: 5 μM) in aqueous buffer.

r of NR (λ_{em} = 625 nm)			**r of NB (λ_{em}** = 665 nm)		
Buffer	**SP10 (10CS10**: 5 μM)	**SP12 (12CS12**: 5 μM)	**Buffer**	**SP10 (10CS10**: 5 μM)	**SP12 (12CS12**: 5 μM)
0.066	0.171	0.183	0.055	0.109	0.104

E. Energy transfer studies of SPs with Rhodamine dyes:

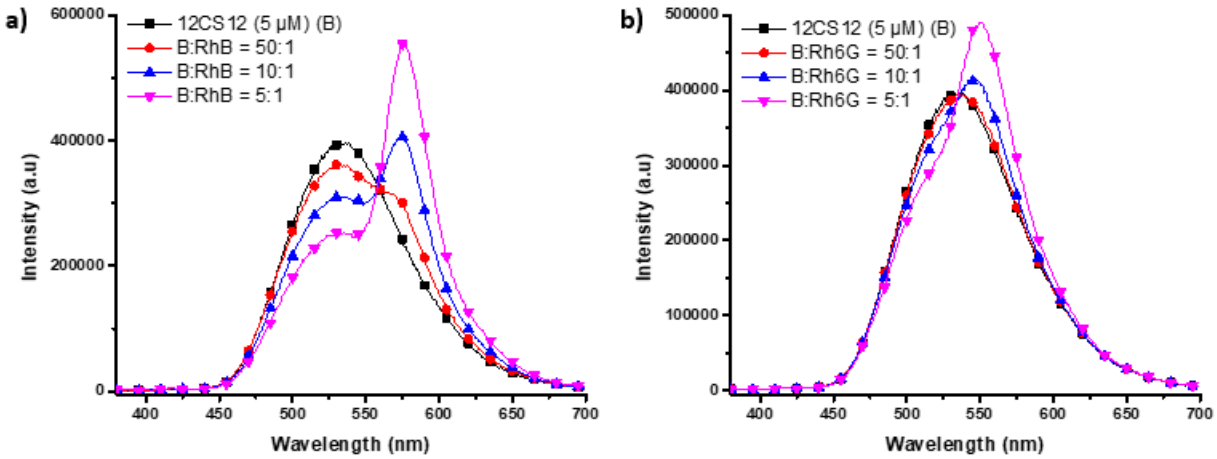

Fig. S16 Emission spectral changes of **SP12 (12CS12**: 5 μM, **B**) upon addition of (a) Rhodamine B (**RhB**) and (b) Rhodamine 6G (**Rh6G**) at different donor/acceptor ratios in aqueous buffer (5 mM tris-HCl, 99:1 water-DMSO).

Table S12. Values of ET efficiency (%) in **SP12-RhB** and **SP12-Rh6G** (**12CS12**: 5 μM) at different donor/acceptor ratio.

Donor/acceptor ratio	For RhB	For Rh6G
50:1	9.6%	2.7%
10:1	22%	6.7%
5:1	36.5%	12%

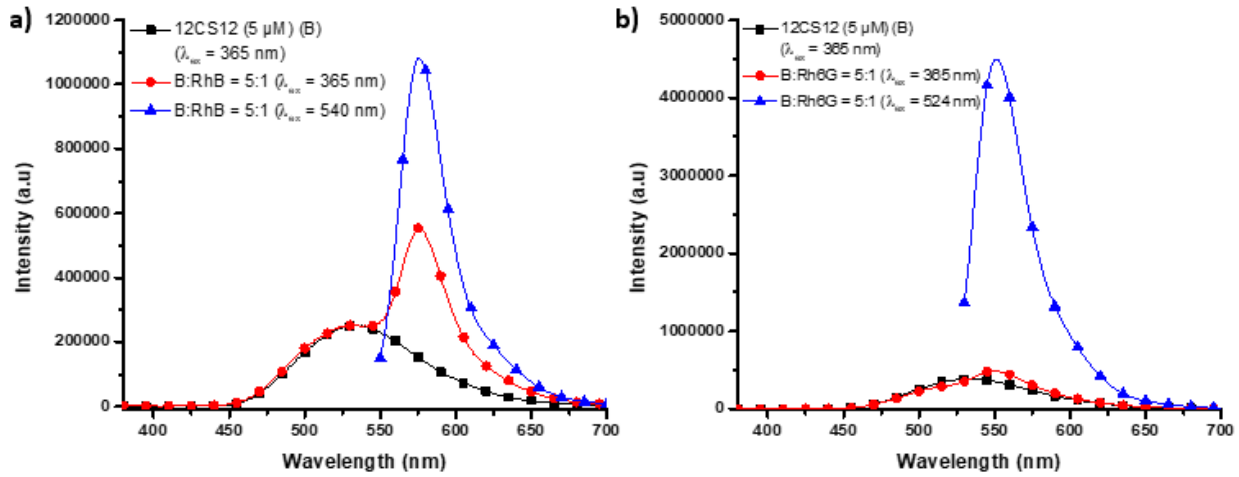

Fig. S17 Emission spectra of **12CS12** (5 μM, **B**) in aqueous buffer in presence of (a) Rhodamine B (**RhB**) and (b) Rhodamine 6G (**Rh6G**) at 5:1 donor/ acceptor ratio. Red trace: donor emission (λ_{ex} = 365 nm) and blue trace: acceptor emission (λ_{ex} = 586 nm). Black trace represents emission spectrum of **12CS12** (5 μM) (λ_{ex} = 365 nm) which was normalized to the intensity at 540 nm of the red trace.

Table S13. Antenna effect (AE) values of **SP12 (12CS12**: 5 μM) to Rhodamine B (**RhB**) and Rhodamine 6G (**Rh6G**) at donor/acceptor ratio of 5:1

Donor/acceptor ratio	In presence of RhB	In presence of Rh6G
5:1	0.38	0.032

3. Energy Transfer Studies of HSPs in Aqueous Buffer:

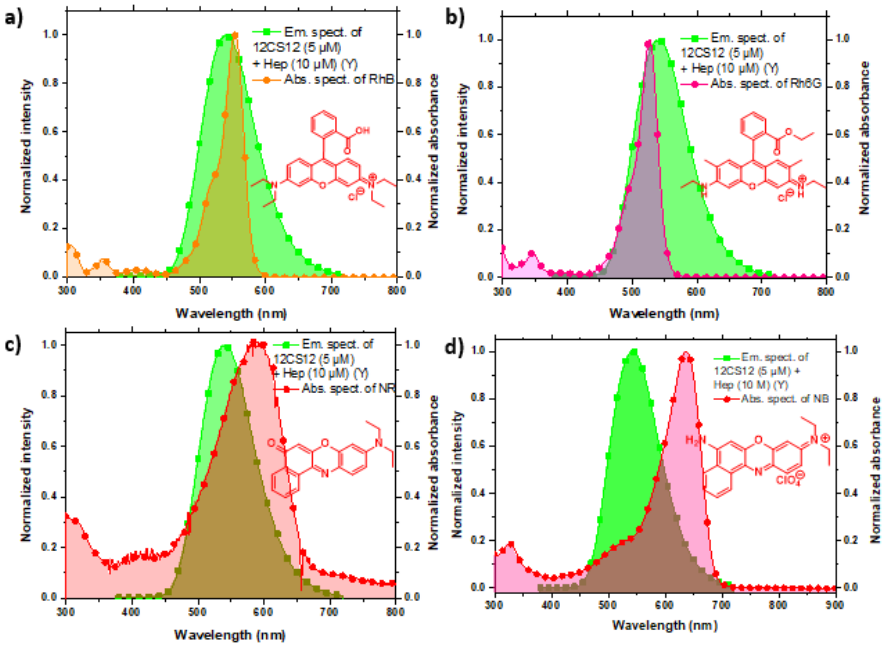

Fig. S18 Spectral overlap of emission of **HSP12** [**12CS12** (5 μM)-heparin (10 μM), **Y**] and absorption of (a) Rhodamine B (**RhB**), (b) Rhodamine 6G (**Rh6G**), (c) Nile Red (**NR**) and (d) Nile Blue (**NB**) in aqueous buffer (5 mM tris-HCl, 99:1 water/DMSO, pH 7.40).

A. Spectral overlap between HSP12 and acceptor dyes:

The overlap integral [$J(\varepsilon)$] for emission spectra of **HSP12** [**12CS12** (5 μM)-heparin (10 μM), **Y**] and absorption spectra of the acceptor dyes were calculated by FluorTools software.

Table S14. Overlap integral [$J(\varepsilon)$] for emission spectra of **HSP12** [**12CS12** (5 μM)-heparin (10 μM), **Y**] and absorption spectra of the acceptor dyes

Rhodamine B (RhB)	Rhodamine 6G (Rh6G)	Nile Red (NR)	Nile Blue (NB)
7.50×10^{-13} $M^{-1}cm^3$	1.15×10^{-13} $M^{-1}cm^3$	8.24×10^{-14} $M^{-1}cm^3$	3.64×10^{-13} $M^{-1}cm^3$

B. Calculation for radiative rate constant (k_r) for HSP12:

Radiative rate constant (k_r) of donor in **HSP12** [**12CS12** (5 μM)-heparin (10 μM)] is calculated using following equation

$k_r = Q_D/\tau$

where, Q_D = Quantum efficiency of donor = 0.224 for **HSP12** [**12CS12** (5 μM)-heparin (10 μM)]

τ = Average lifetime of the donor in **HSP12** [**12CS12** (5 μM)-heparin (10 μM)] = 9.98 ns

Radiative rate constant (k_r) of **HSP12** [**12CS12** (5 μM)-heparin (10 μM)] is determined to be 2.24×10^7 s^{-1}

C. Förster radius (R_0) calculation for HSP12-NR:

For any FRET system, Förster Radius (R_0) is calculated by using the following equation-

$$R_0 = 9.78 \times 10^3 \times [k^2 \times n^{-4} \times Q_D \times J(\varepsilon)]^{1/6} \text{ in Å}$$

where,

k^2 = Relative orientation in space of the transition dipoles of donor and acceptors which is usually assumed to be 2/3.
n = refractive index of the medium = 1.33 for aqueous buffer
Q_D = Quantum efficiency of donor = 0.224 for **HSP12** [**12CS12** (5 μM)-heparin (10 μM)]
$J(\varepsilon)$ = Overlap integral of emission spectra of donor **HSP12** [**12CS12** (5 μM)-heparin (10 μM)] and absorption spectra of acceptor [Nile Red (**NR**)] = 8.24×10^{-14} $M^{-1}cm^3$

R_0 for **HSP12** [**12CS12** (5 μM)-heparin (10 μM)]- **NR** was calculated to be 38.9 Å (~3.9 nm).

D. Energy transfer studies of HSPs to Nile Red (NR) and Nile Blue (NB):

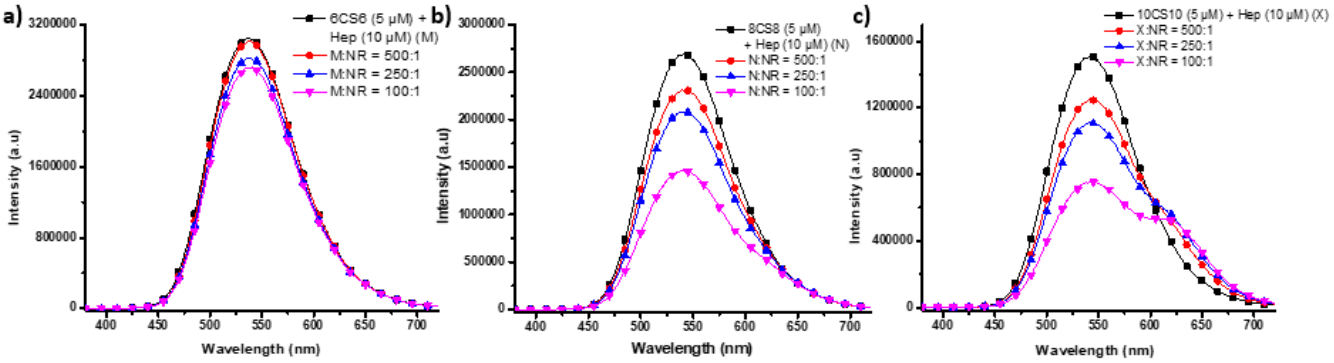

Fig. S19 Emission spectral changes of (a) **HC6** [**6CS6** (5 μM)-heparin (10 μM), **M**], (b) **HSP8** [**8CS8** (5 μM)-heparin (10 μM), **N**] and (c) **HSP10** [**10CS10** (5 μM)-heparin (10 μM), **X**] upon addition of Nile Red (**NR**) in aqueous buffer (5 mM tris-HCl, 99:1 water-DMSO).

Table S15. Values of ET efficiency (%) from **HC6 and HSP**s to Nile Red (**NR**) at different donor/acceptor ratio.

Donor/acceptor ratio	HSP8 [8CS8 (5 μM)-heparin (10 μM)]	HSP10 [10CS10 (5 μM)-heparin (10 μM)]	HSP12 [12CS12 (5 μM)-heparin (10 μM)]	HC6 [6CS6 (5 μM)-heparin (10 μM)]
1000:1	-	-	19.40%	-
500:1	14.47%	17.33%	37.64%	1.53%
250:1	22.72%	26.40%	60.00%	7.55%
100:1	45.75%	50.00%	80.30%	11.40%

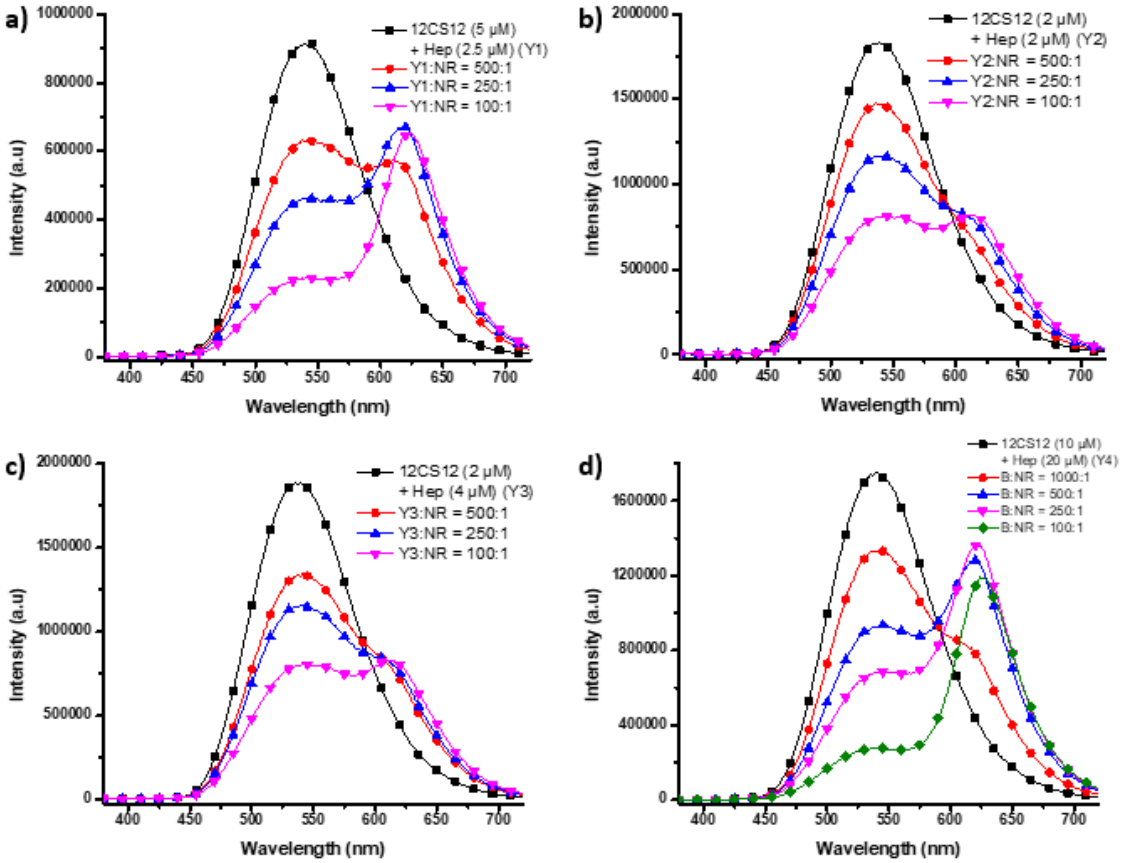

Fig. S20 Emission spectral changes of **HSP12** having different composition of **12CS12** and heparin upon addition of Nile Red (**NR**) in aqueous buffer (5 mM tris-HCl, 99:1 water-DMSO). (a) **12CS12** (5 μM)-heparin (2.5 μM) (**Y1**), (b) **12CS12** (2 μM)-heparin (2 μM) (**Y2**) and (c) **12CS12** (2 μM)-heparin (4 μM) (**Y3**) and (d) **12CS12** (10 μM)-heparin (20 μM) (**Y4**).

Table S16. ET efficiency (%) from **HSP12** to Nile Red (**NR**) at different donor/acceptor ratios.

Donor/acceptor ratio	HSP12 [12CS12 (5 μM)-heparin (2.5 μM), Y1]	HSP12 [12CS12 (2 μM)-heparin (2 μM), Y2]	HSP12 [12CS12 (2 μM)-heparin (4 μM), Y3]	HSP12 [12CS12 (10 μM)-heparin (20 μM), Y4]
500:1	31.03%	19.53%	29.70%	47.35%
250:1	49.30%	36.60%	38.77%	61.20%
100:1	74.79%	56.00%	57.80%	84.30%

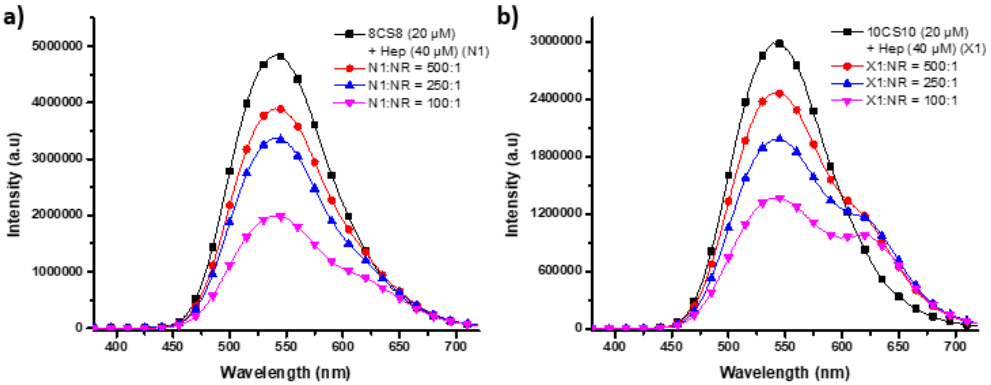

Fig. S21 Emission spectral changes of (a) **HSP8** [**8CS8** (20 μM)-heparin (40 μM), **N1]** and (b) **HSP10** [**10CS10** (20 μM)-heparin (40 μM), **X1**] upon addition of Nile Red (**NR**) in aqueous buffer (5 mM tris-HCl, 99:1 water-DMSO).

Table S17. ET efficiency (%) from **HSP8** and **HSP10** to Nile Red (**NR**) at different donor/acceptor ratio.

Donor/acceptor ratio	HSP8 [8CS8 (20 μM)-heparin (40 μM), N1]	HSP10 [10CS10 (20 μM)-heparin (40 μM), Y1]
500:1	17.35%	29.70%
250:1	30.56%	33.77%
100:1	56.00%	57.80%

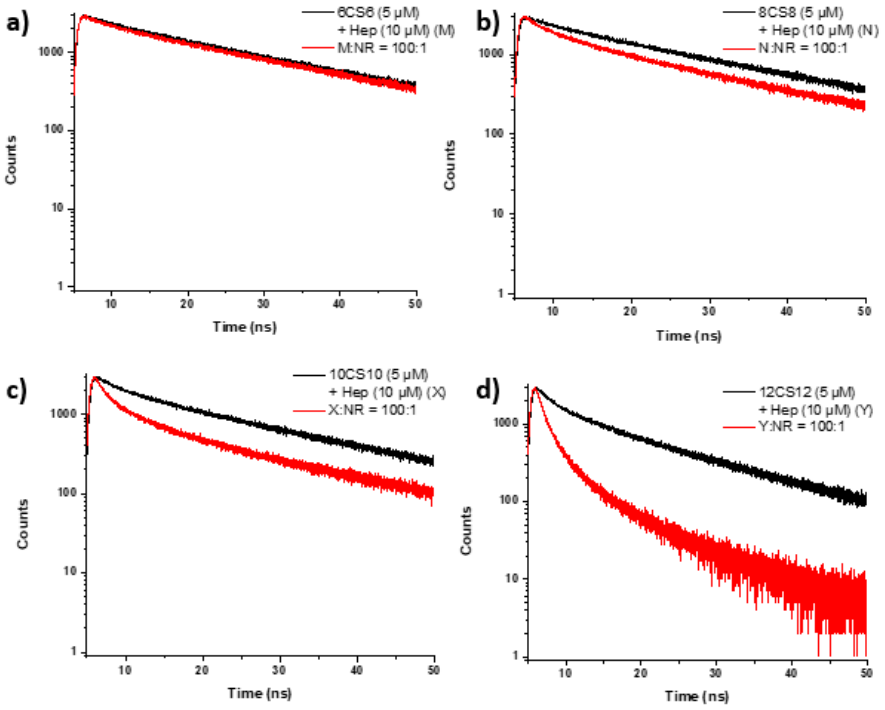

Fig. S22 Time-resolved fluorescence decay curves of (a) **HC6** [**6CS6** (5 μM)-heparin (10 μM), **M**], (b) **HSP8** [**8CS8** (5 μM)-heparin (10 μM), **N**], (c) **HSP10** [**10CS10** (5 μM)-heparin (10 μM), **X**] and (d) **HSP12** [**12CS12** (5 μM)-heparin (10 μM), **Y**] upon addition of Nile Red (**NR**) at donor/acceptor ratio of 100:1 in aqueous buffer.

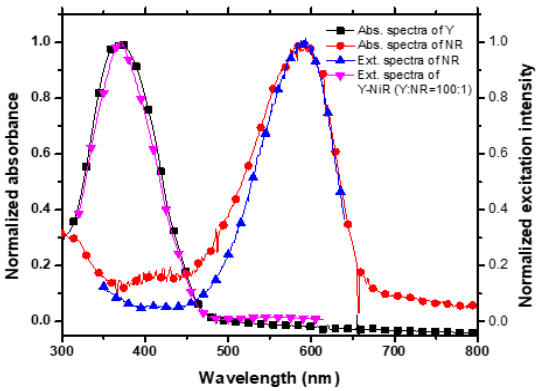

Fig. S23 Normalized absorption spectra of **HSP12** [**12CS12** (5 μM)-heparin (10 μM), **Y**], Nile Red (**NR**) and normalized excitation spectra of **HSP12** [**12CS12** (5 μM)-heparin (10 μM), **Y**], Nile Red (**NR**) in aqueous buffer.

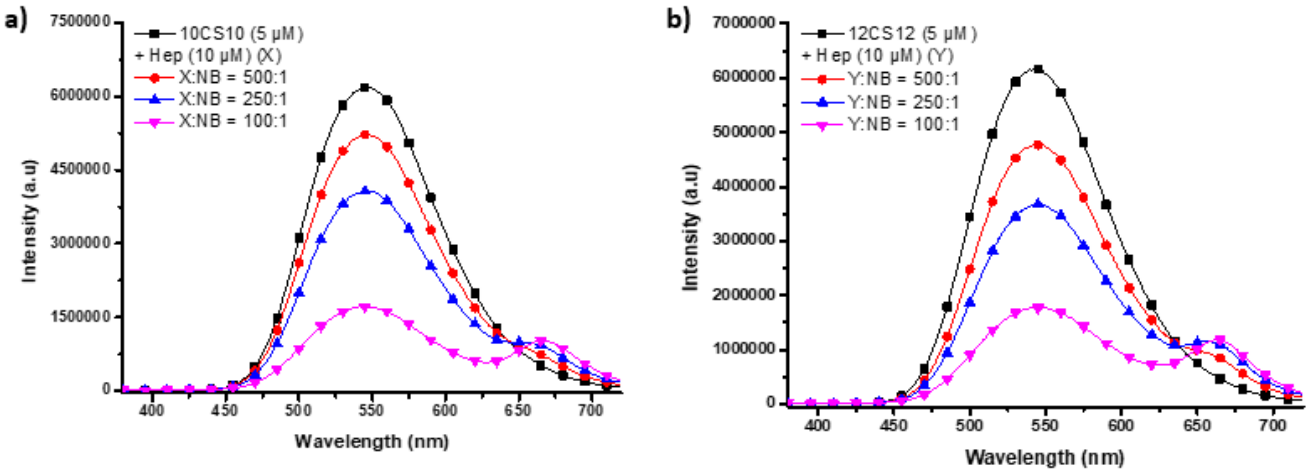

Fig. S24 Emission spectral changes of (a) **HSP10** [**10CS10** (5 μM)-heparin (10 μM), **X**] and (b) **HSP12** [**12CS12** (5 μM)-heparin (10 μM), **Y**] upon addition of Nile Blue (**NB**) in aqueous buffer (5 mM tris-HCl, 99:1 water-DMSO).

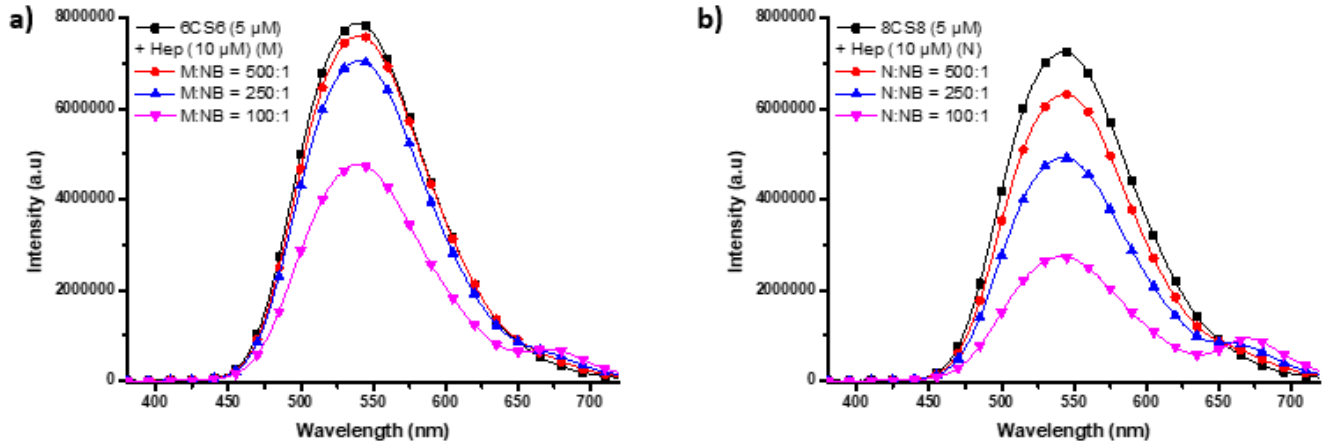

Fig. S25 Emission spectral changes of (a) **HC6** [**6CS6** (5 μM)-heparin (10 μM), **M**] and (b) **HSP8** [**8CS8** (5 μM)-heparin (10 μM), **N**] upon addition of Nile Blue (**NB**) in aqueous buffer (5 mM tris-HCl, 99:1 water-DMSO).

Table S18. ET efficiency (%) from **HSP**s and **HC6** to Nile Blue (**NB**) at different donor/acceptor ratios.

Donor/acceptor ratio	HSP8 [8CS8 (5 μM)-heparin (10 μM)]	HSP10 [10CS10 (5 μM)-heparin (10 μM)]	HSP12 [12CS12 (5 μM)-heparin (10 μM)]	HC6 [6CS6 (5 μM)-heparin (10 μM)]
500:1	13%	16%	23%	4%
250:1	32%	34%	40.5%	11%
100:1	62%	72%	71%	40%

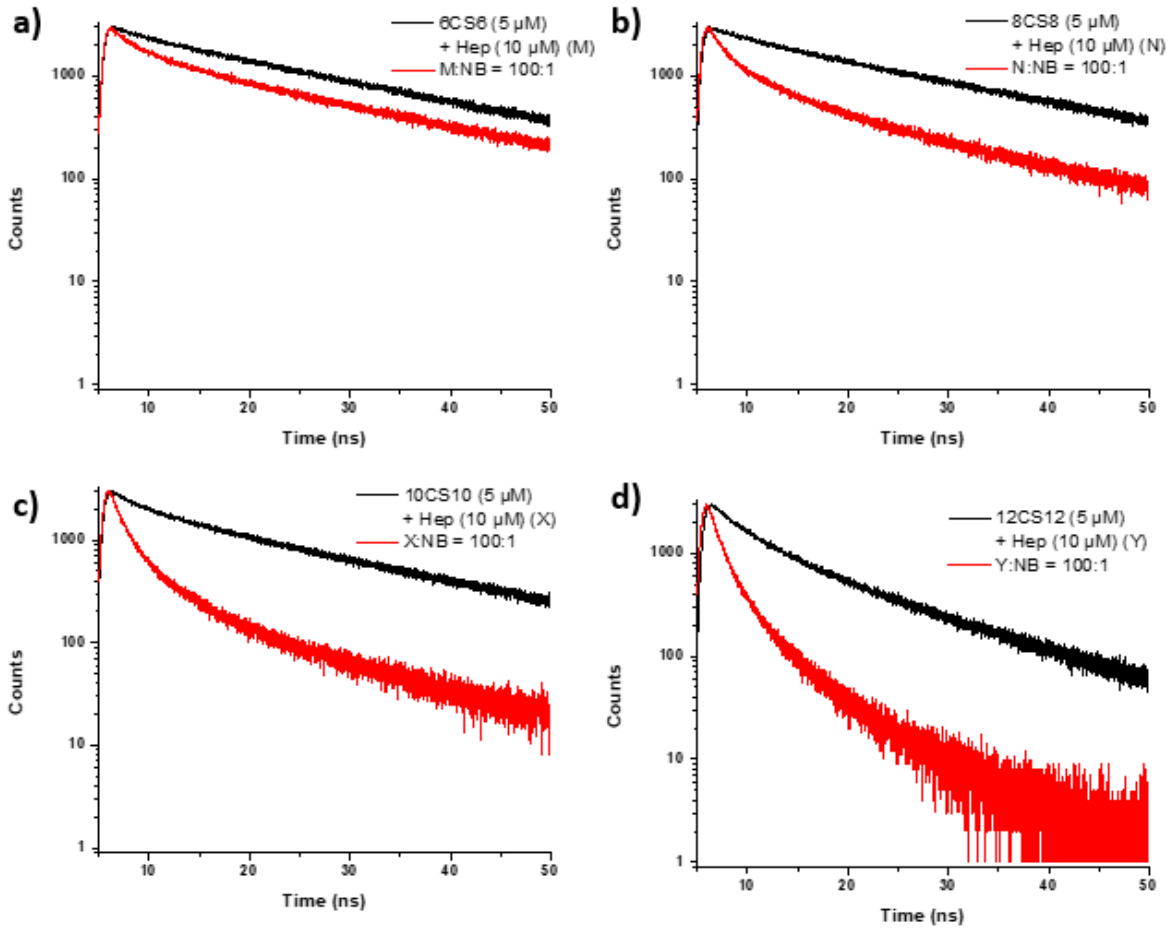

Fig. S26 Time-resolved fluorescence decay curves of (a) **HC6 [6CS6 (5 μM)-heparin (10** μM), **M**], (b) **HSP8** [**8CS8** (5 μM)-heparin (10 μM), **N**], (c) **HSP10** [**10CS10** (5 μM)-heparin (10 μM), **X**] and (d) **HSP12** [**12CS12** (5 μM)-heparin (10 μM), **Y**] upon addition of Nile Blue (**NB**) at donor/acceptor ratio of 100:1 in aqueous buffer.

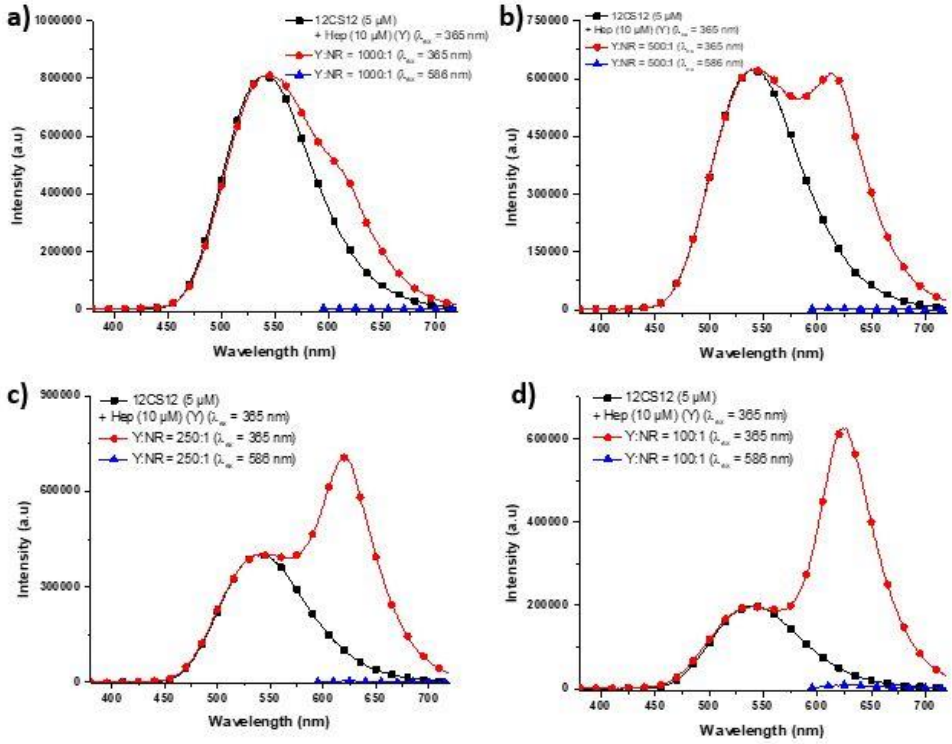

Fig. S27 Emission spectra of **HSP12** [**12CS12** (5 μM)-heparin (10 μM), **Y**]-**NR** in aqueous buffer at (a) 1000:1, (b) 500:1, (c) 250:1 and (d) 100:1 donor/ acceptor ratios. Red trace: donor emission (λ_{ex} = 365 nm) and blue trace: acceptor emission (λ_{ex} = 586 nm). Black trace represents emission spectrum of **HSP12** [**120CS12** (5 μM)-heparin (10 μM), **Y**] (λ_{ex} = 365 nm) which was normalized to the intensity at 540 nm of the red trace.

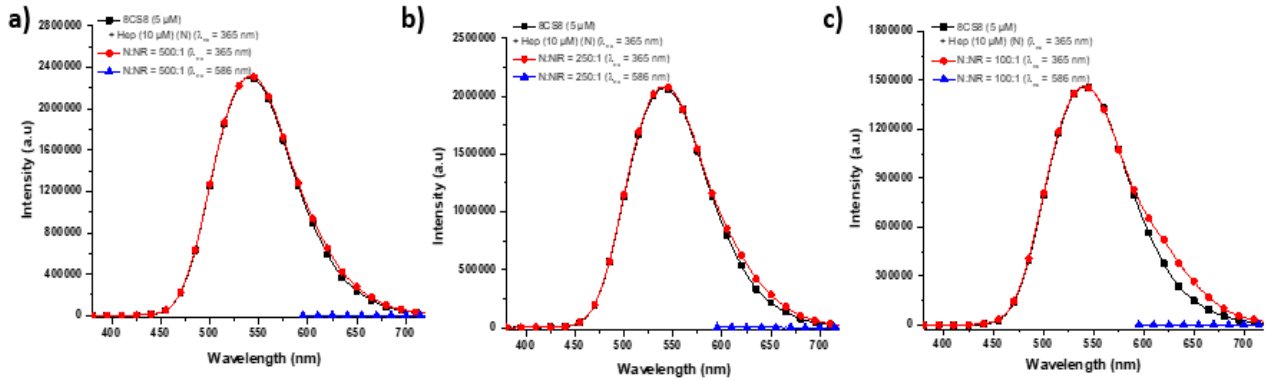

Fig. S28 Emission spectra of **HSP8** [**8CS8** (5 μM)-heparin (10 μM), **N**]-**NR** in aqueous buffer at (a) 500:1, (b) 250:1 and (c) 100:1 donor/ acceptor ratios Red trace: donor emission (λ_{ex} = 365 nm) and blue trace: acceptor emission (λ_{ex} = 586 nm). Black trace represents emission spectrum of **HSP8** [**8CS8** (5 μM)-heparin (10 μM), **N**] in **HSP8** (λ_{ex} = 365 nm) which was normalized to the intensity at 540 nm of the red trace.

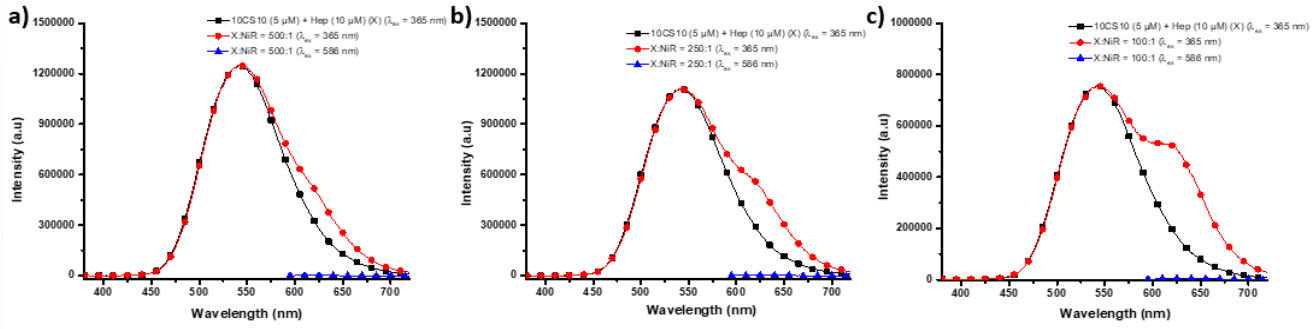

Fig. S29 Emission spectra of **HSP10** [**10CS10** (5 μM)-heparin (10 μM), **X**] in aqueous buffer at (a) 500:1, (b) 250:1 and (c) 100:1 donor/ acceptor ratios. Red trace: donor emission (λ_{ex} = 365 nm) and blue trace: acceptor emission (λ_{ex} = 586 nm). Black trace represents emission spectrum of **HSP10** [**10CS10** (5 μM)-heparin (10 μM), **X**] (λ_{ex} = 365 nm) which was normalized to the intensity at 540 nm of the red trace.

Table S19. Antenna effect (AE) values in **HSP**-**NR** and **HC6**-**NR** triads at different donor/acceptor ratio.

Donor/acceptor ratio	HSP12 [12CS12 (5 μM)-Heparin (10 μM)]	HSP8 [8CS8 (5 μM)-Heparin (10 μM)]	HSP10 [10CS10 (5 μM)-Heparin (10 μM)]	HC6 [6CS6 (5 μM)- Heparin (10 μM)]
1000:1	97	-	-	-
500:1	149	62	81	3
250:1	124	64	86	11
100:1	66	76	72	11

Table S20. Antenna effect (AE) values in **HSP12**-**NR** triad at different donor/acceptor ratio.

Donor/acceptor ratio	HSP12 [12CS12 (5 μM)-Heparin (2.5 μM), Y1]	HSP12 [12CS12 (2 μM)-Heparin (2 μM), Y2]	HSP12 [12CS12 (2 μM)-Heparin (4 μM), Y3]	HSP12 [12CS12 (10 μM)-Heparin (20 μM), Y4]
500:1	126	111	149	134
250:1	103	105	130	98
100:1	61	101	117	51

Table S21. Antenna effect (AE) values **HSP8**-**NR** and **HSP10**-**NR** triads at different donor/acceptor ratio.

Donor/acceptor ratio	HSP8 [8CS8 (20 μM)- Heparin (40 μM), N1]	HSP10 [10CS10 (20 μM)- Heparin (40 μM), Y1]
500:1	57	51
250:1	48	46
100:1	46	37

Table S22. Antenna effect (AE) values in **HSP**-**NB** and **HC6**-**NB** triads at different donor/acceptor ratio.

Donor/acceptor ratio	HSP12 [12CS12 (5 μM)-Heparin (10 μM)]	HSP8 [8CS8 (5 μM)-Heparin (10 μM)]	HSP10 [10CS10 (5 μM)-Heparin (10 μM)]	HC6 [6CS6 (5 μM)- Heparin (10 μM)]
500:1	115	53	90	57
250:1	90	63	89	45
100:1	59	47	53	36

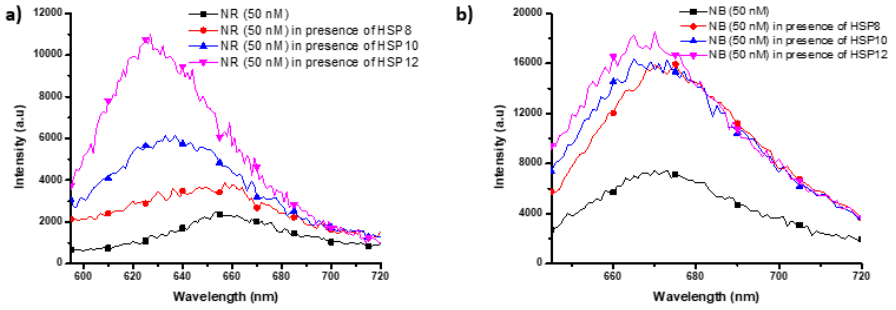

Fig. S30 Emission spectra of (a) Nile Red (**NR**) (50 nM) and (b) Nile Blue (**NB**) (50 nM) in absence and in presence of **HSP**s [**NCSN**: 5 μM, Heparin: 10 μM].

Table S23. Steady-state fluorescence anisotropy values (**r**) of **NR** (50 nM) (λ_{ex} = 586 nm) and **NB** (50 nM) (λ_{ex} = 635 nm) in absence and presence of **HC6** and **HSP**s in aqueous buffer.

Without co-assemblies		HC6 [6CS6 (5 μM)- Heparin (10 μM)]		HSP8 [8CS8 (5 μM)-Heparin (10 μM)]		HSP10 [10CS10 (5 μM)-Heparin (10 μM)]		HSP12 [12CS12 (5 μM)-Heparin (10 μM)]	
r of NR	r of NB	r of NR	r of NB	r of NR	r of NB	r of NR	r of NB	r of NR	r of NB
0.066	0.055	0.06	0.110	0.134	0.211	0.167	0.197	0.176	0.186

Table S24. Steady-state fluorescence anisotropy values of **HSP**s (λ_{ex} = 365 nm, λ_{em} = 540 nm) in absence and presence of **NR** and **NB** in aqueous buffer.

HSP8 [8CS8 (5 μM)- Heparin (10 μM)]			**HSP10 [10CS10 (5 μM)- Heparin (10 μM)]**			**HSP12 [12CS12 (5 μM)- Heparin (10 μM)]**		
W/o- NR	**W/- NR (50 nM)**	**W/- NB (50 nM)**	**W/o- NR**	**W/- NR (50 nM)**	**W/- NB (50 nM)**	**W/o- NR**	**W/- NR (50 nM)**	**W/- NB (50 nM)**
0.057	0.062	0.051	0.103	0.106	0.124	0.123	0.144	0.145

Table S25. Steady-state fluorescence anisotropy values (**r**) of **NR** (50 nM) and **NB** λ_{ex} = 365 nm) in presence of **HSP**s in aqueous buffer.

HSP8 [8CS8 (5 μM)- Heparin (10 μM)]		**HSP10 [10CS10 (5 μM)- Heparin (10 μM)]**		**HSP12 [12CS12 (5 μM)- Heparin (10 μM)]**	
r of NR	**r of NB**	**r of NR**	**r of NB**	**r of NR**	**r of NB**
0.037	0.014	0.056	0.068	0.078	0.067

E. Determination of the number of donors per acceptor in an antenna.

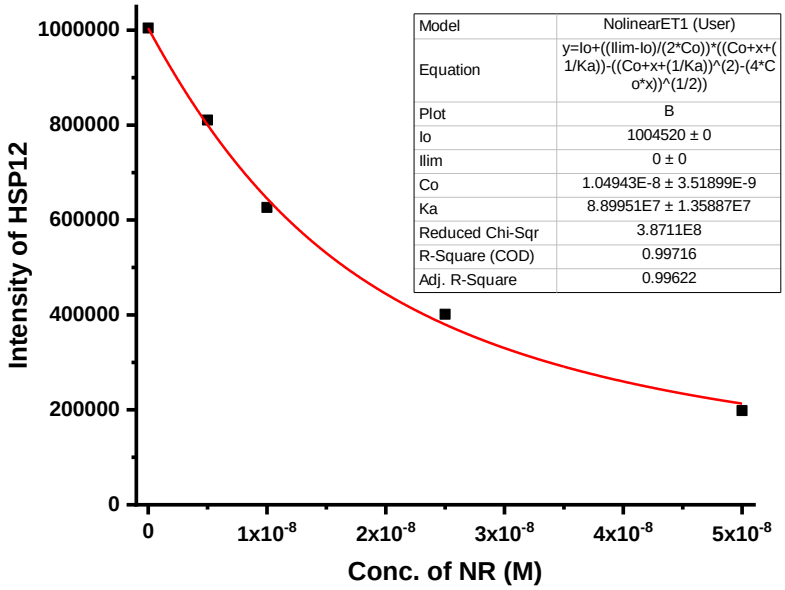

Fig. S31 Non-linear fitting of the emission intensities of **HSP12** [**12CS12**: 5 μM; heparin: 10 μM] versus the concentration of **NR**.

In the antenna, donor emission was quenched upon the addition of the acceptor (**NR**). As both dynamic and static quenching can participate quenching of donor emission, a model that combines both mechanisms was used to calculate the number of donor (*n*) value in an antenna. We assumed that one light-harvesting antenna binds with one acceptor by a 1:1 binding isotherm. Therefore, the expression for the model can be written in the following form-

$(Donor)_n + Acceptor = (Donor)_n–Acceptor$

On this basis, a donor quenching model was employed, which can be expressed by the following equation[S3]

$$I_F = I_0 + ((I_{lim} - I_0)/2c_0) \times ((c_0 + c_A + 1/K_a) - ((c_0 + c_A + 1/K_a)^2 - 4c_0c_A)^{1/2})$$

In this equation, I_F is the fluorescent emission intensity of the **CS** nanotubes in presence of the acceptor with a known concentration. I_0 is the emission intensity in absence of the acceptor. I_{lim} is the emission intensity limitation of the system in presence of the acceptor ($I_{lim} \rightarrow 0$). c_0 denotes the concentration of donor assembly $(Donor)_n$, while c_A is the concentration of acceptor. K_a is the association constant on the basis of the 1:1 binding model. From the equation, c_0 and K_a were obtained. The number of donors (n) present in the antenna was calculated using the formula $n = c_D/c_0$, where c_D is the total donor concentration and the value of n was calculated to be 516±182.

E. Energy transfer studies of HSPs with Rhodamine dyes:

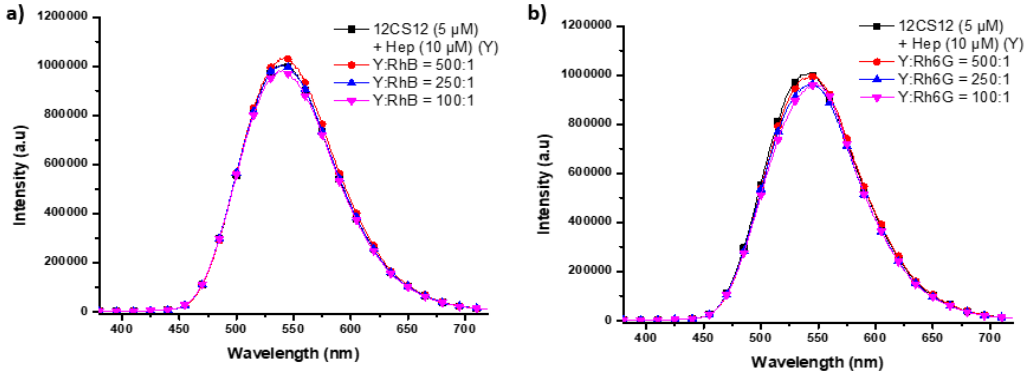

Fig. S32 Emission spectral changes of **HSP12** [**12CS12** (5 μM)-heparin (10 μM), **Y**] upon addition of (a) Rhodamine B (**RhB**) and (b) Rhodamine 6G (**Rh6G**) up to donor/acceptor ratio of 100:1 in aqueous buffer (5 mM tris-HCl, 99:1 water-DMSO).

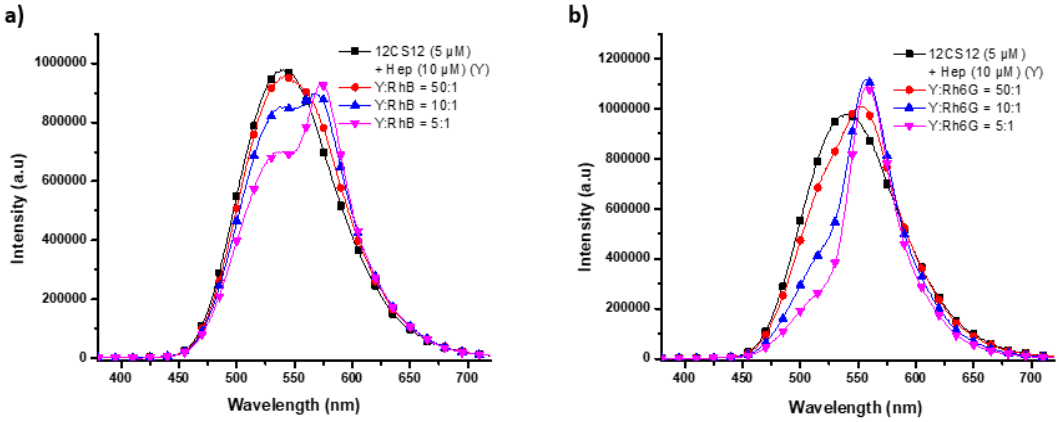

Fig. S33 Emission spectral changes of of **HSP12** [**12CS12** (5 μM)-heparin (10 μM), **Y**] upon addition of (a) Rhodamine B (**RhB**) and (b) Rhodamine 6G (**Rh6G**) at higher donor/acceptor ratios in aqueous buffer (5 mM tris-HCl, 99:1 water-DMSO).

Table S26. Values of ET efficiency (%) of **HSP12** [**12CS12** (5 μM)-heparin (10 μM), **Y**] to Rhodamine B (**RhB**) and Rhodamine 6G (**Rh6G**) at different donor/acceptor ratio.

Donor/acceptor ratio	In presence of RhB	In presence of Rh6G
50:1	3%	4.9%
10:1	13.3%	22%
5:1	28.6%	34.8%

Table S27. Antenna effect (AE) values of **HSP12** [**12CS12** (5 µM)-heparin (10 µM), **Y**] to Rhodamine B (**RhB**) and Rhodamine 6G (**Rh6G**) at donor/acceptor ratio of 5:1.

Donor/acceptor ratio	In presence of RhB	In presence of Rh6G
5:1	0.31	0.16

Table S28. Anisotropy values of Rhodamine dyes (50 nM) in presence of **HSP12** [**12CS12** (5 µM)-heparin (10 µM), **Y**] in aqueous buffer.

RhB	Rh6G
0.015	0.037

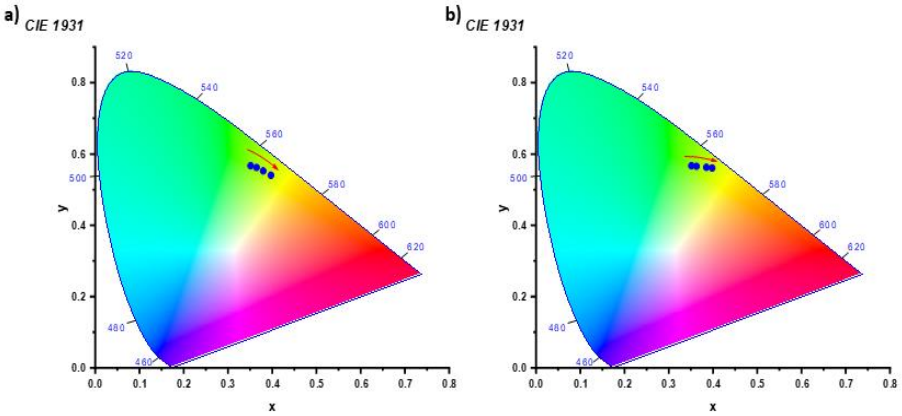

Fig. S34 CIE diagram displaying colour transition of **HSP12** [**12CS12** (5 µM)-heparin (10 µM), **Y**] from greenish yellow to yellow upon addition of (a) **RhB** (0 to 0.2 eq.) and (b) **Rh6G** (0 to 0.2 eq.) in aqueous buffer (5 mM tris-HCl, 99:1 water-DMSO).

4. Demonstration of Fluorescent Thermometer:

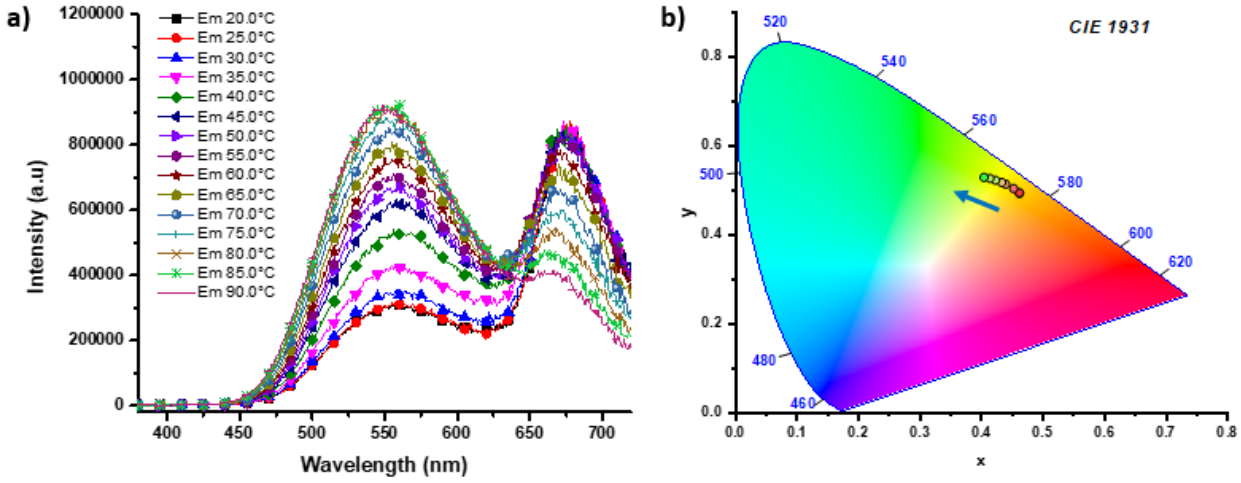

Fig. S35 (a) Emission changes of **HSP12-NB** [**12CS12**: 5 µM; heparin: 10 µM; **NB**: 100 nM] at different temperatures demonstrating fluorescence thermometer application. (b) CIE co-ordinates for the plots in (a).

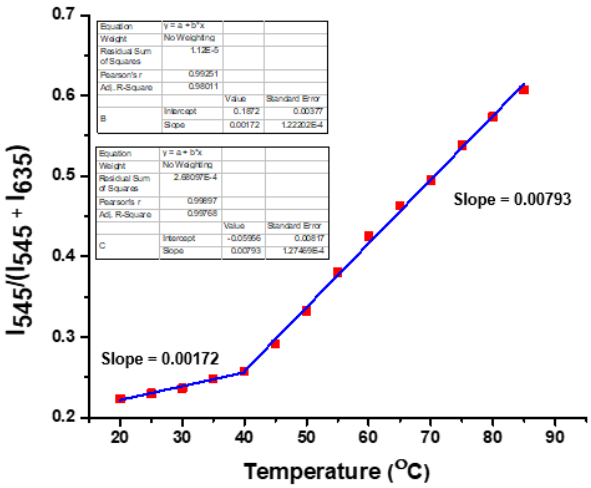

Fig. S36 Linear fitted plot of $I_{545}/(I_{545}+I_{635})$ vs temperature (for **HSP12-NR**) in aqueous buffer.

5. Energy Transfer Studies of SP12 and HSP12 in Film State Made from Aqueous Solution:

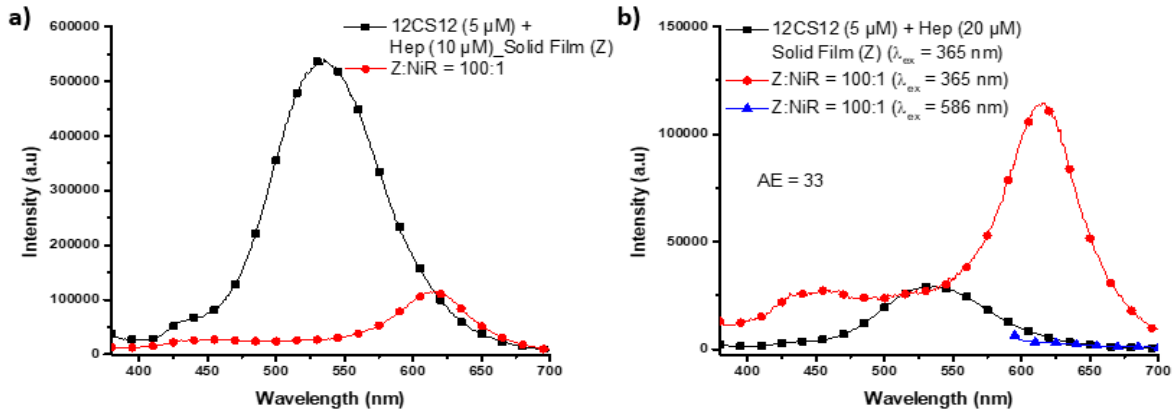

Fig. S37 (a) Emission spectral changes of **HSP12** [**12CS12** (5 μM)-heparin (10 μM), **Z**] upon addition of Nile Red (**NR**) (D/A ratio = 100:1) in solid film. (b) Emission spectra of **HSP12** [**12CS12** (5 μM)-heparin (10 μM), **Z**]-**NR** in film state at 100:1 donor/ acceptor ratio. Red trace: donor emission (λ_{ex} = 365 nm) and blue trace: acceptor emission (λ_{ex} = 586 nm). Black trace represents emission spectrum of **HSP12** [**12CS12** (5 μM)-heparin (10 μM), **Z**] (λ_{ex} = 365 nm) in film state which was normalized to the intensity at 540 nm of the red trace.

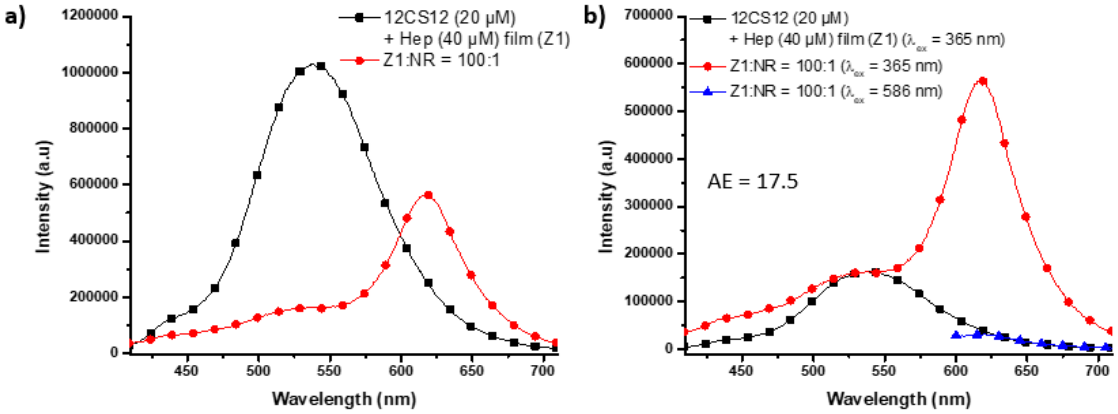

Fig. S38 (a) Emission spectral changes of **HSP12** [**12CS12** (20 μM)-heparin (40 μM), **Z1**] upon addition of Nile Red (**NR**) (D/A ratio = 100:1) in solid film. (b) Emission spectra of **HSP12** [**12CS12** (20 μM)-heparin (40 μM), **Z1**]-**NR** in film state at 100:1 donor/ acceptor ratio. Red trace: donor emission (λ_{ex} = 365 nm) and blue trace: acceptor emission (λ_{ex} = 586 nm). Black trace represents emission spectrum of **HSP12** [**12CS12** (20 μM)-heparin (40 μM), **Z1**] (λ_{ex} = 365 nm) in film state which was normalized to the intensity at 540 nm of the red trace.

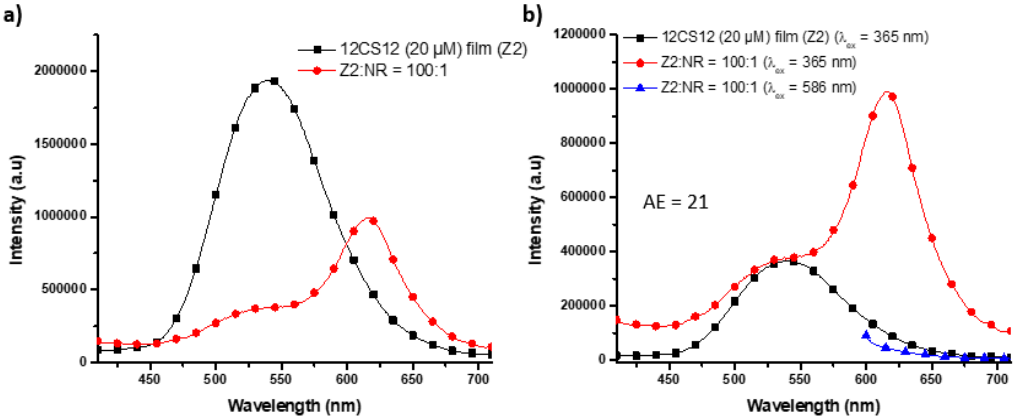

Fig. S39 (a) Emission spectral changes of **SP12** [**12CS12:** 20 μM) (**Z2**)] upon addition of Nile Red (**NR**) (D/A ratio = 100:1) in solid film. (b) Emission spectra of **SP12** [**12CS12:** 20 μM) (**Z2**)]**-NR** in film state at 100:1 donor/ acceptor ratio. Red trace: donor emission (λ_{ex} = 365 nm) and blue trace: acceptor emission (λ_{ex} = 586 nm). Black trace represents emission spectrum of **SP12** [**12CS12:** 20 μM) (**Z2**)] (λ_{ex} = 365 nm) in film state which was normalized to the intensity at 540 nm of the red trace.

6. Generation of Multiple Fluorescent Color:

Multiple colors in solid and solution state were prepared as follows-

Fig. 7d: Yellow and red-colored solid films were made from dried **HSP12** (**12CS12:** 10 μM, Heparin: 40 μM) and **HSP12-NR** (200 nM) in buffer respectively.

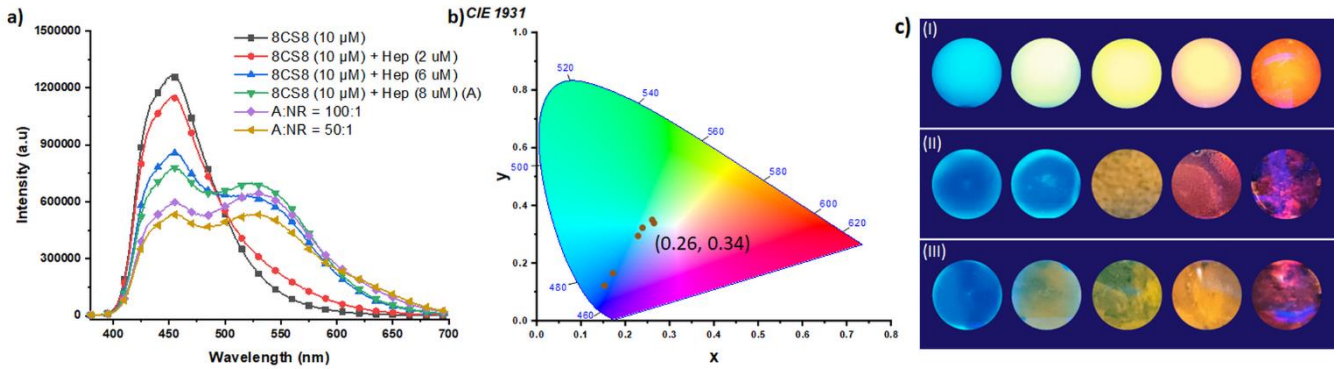

Fig. S40 (a) Emission spectral changes of **8CS8** (10 μM) in PAA (10 mg/mL in buffer) upon addition of Heparin and then Nile Red (**NR**) and (b) corresponding CIE diagram. (c) A range of fluorescence colors using ET made in PAA and in buffer solution (I) without drying, (II) after drying, and (III) after the addition of water to the dried films.

Fig. 7e: Greenish-yellow and white luminescence were generated using **HSP8** (**8CS8**:10 μM, Heparin: 8 μM) and **HSP8-NR** (**8CS8**:10 μM, Heparin: 8 μM, **NR**: 200 nM, D/A = 500:1) respectively from blue fluorescent solution of **8CS8** (10 μM) in PAA (10 mg/mL in buffer). CIE co-ordinate of the white emission was (0.26, 0.34).

Fig. S39c: First two consecutive solution state colors (bluish cyan and yellowish-green respectively) were prepared using (i) **8CS8** (20 μM) and (ii) **HSP8** (**8CS8**: 20 μM), Heparin: 15 μM) respectively in PAA (10 mg/mL in buffer). **8CS8** was chosen as it displayed monomeric bluish cyan in PAA solution in buffer. However, we could modify its color from cyan to yellowish-green upon formation of co-assembly with heparin.
The last three consecutive solution state colors were prepared using (i) **HSP12** (**12CS12**: 20 μM, Heparin: 40 μM), (ii) **HSP12-NR** (**12CS12**: 20 μM, Heparin: 40 μM, **NR**: 50 nM, D/A = 400:1) and (iii) **HSP12-NR** (**12CS12**: 20 μM, Heparin: 40 μM, **NR**: 100 nM, DA = 200:1) in buffer respectively.
Upon drying the colors obtained were bluish, bluish cyan, yellow, orange, and red in solid amorphous films. Upon addition of water, their solution state colors were almost regained.

Fig. 7f: The number 10710 was written in a glass surface using following-

1=> **8CS8** (10 μM) in PAA (10 mg/mL in buffer).

0=> **HSP8-NR** (**8CS8**:10 μM, Heparin:8 μM, **NR**: 200 nM, D/A = 500:1) in PAA (10 mg/mL in buffer).

7=> **HSP12** (**12CS12**: 20 μM, Heparin: 40 μM) in buffer

1=> **HSP12-NR** (**12CS12**: 20 µM, Heparin: 40 µM, **NR**: 80 nM, D/A = 250:1) in buffer.

0=> **HSP12-NR** (**12CS12**: 20 µM, Heparin: 40 µM, **NR**: 200 nM, D/A = 100:1) in buffer.

7. NMR Spectra and MS of the Compounds:

A. ^{1}H NMR spectra of 6CS6 (400 MHz, DMSO-D_6):

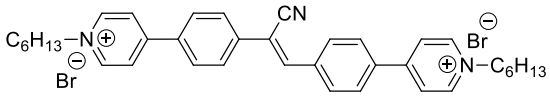

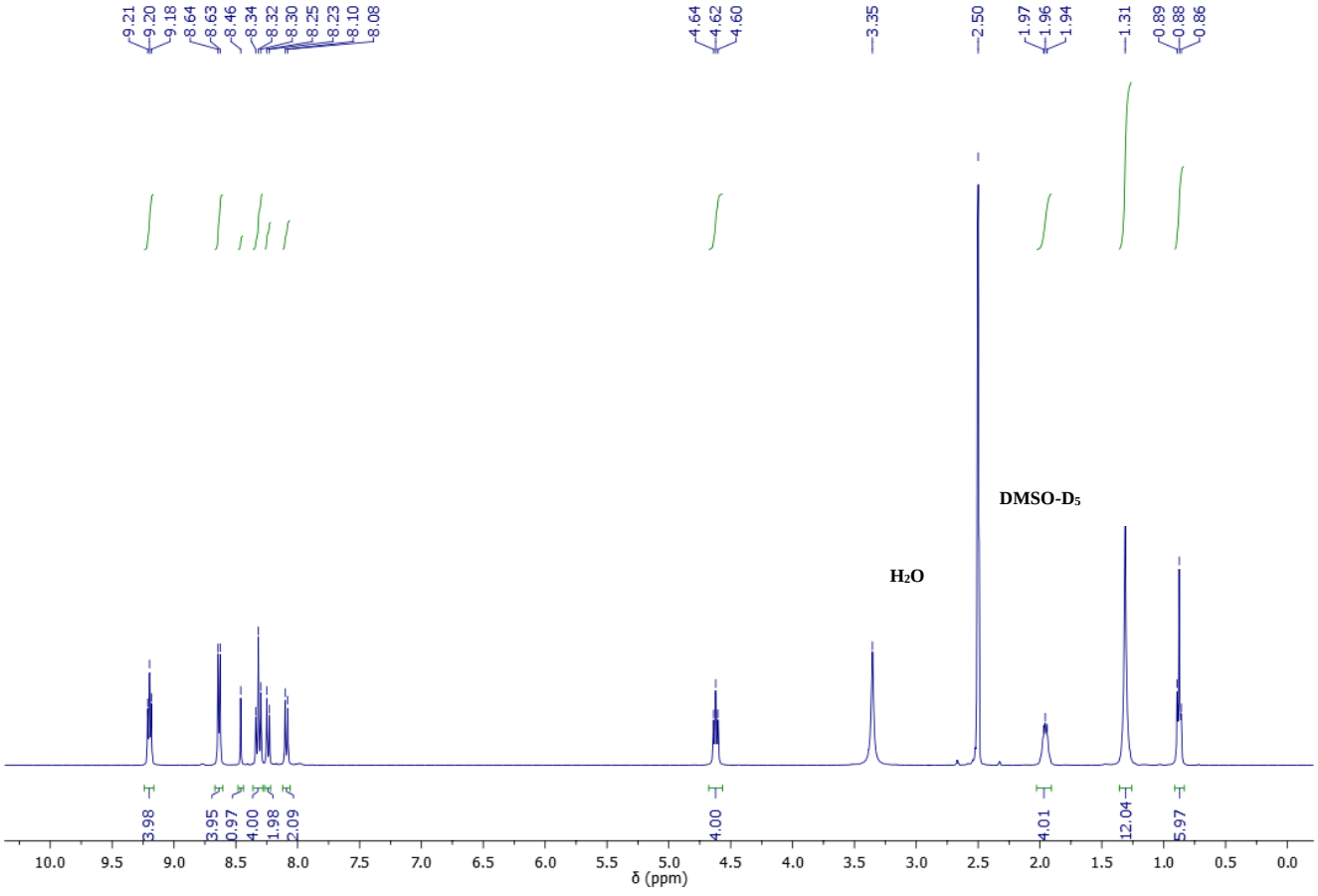

B. ^{13}C NMR spectra of 6CS6 (125 MHz, DMSO-D_6):

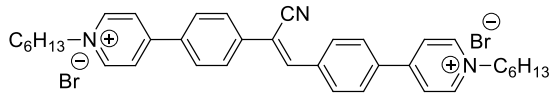

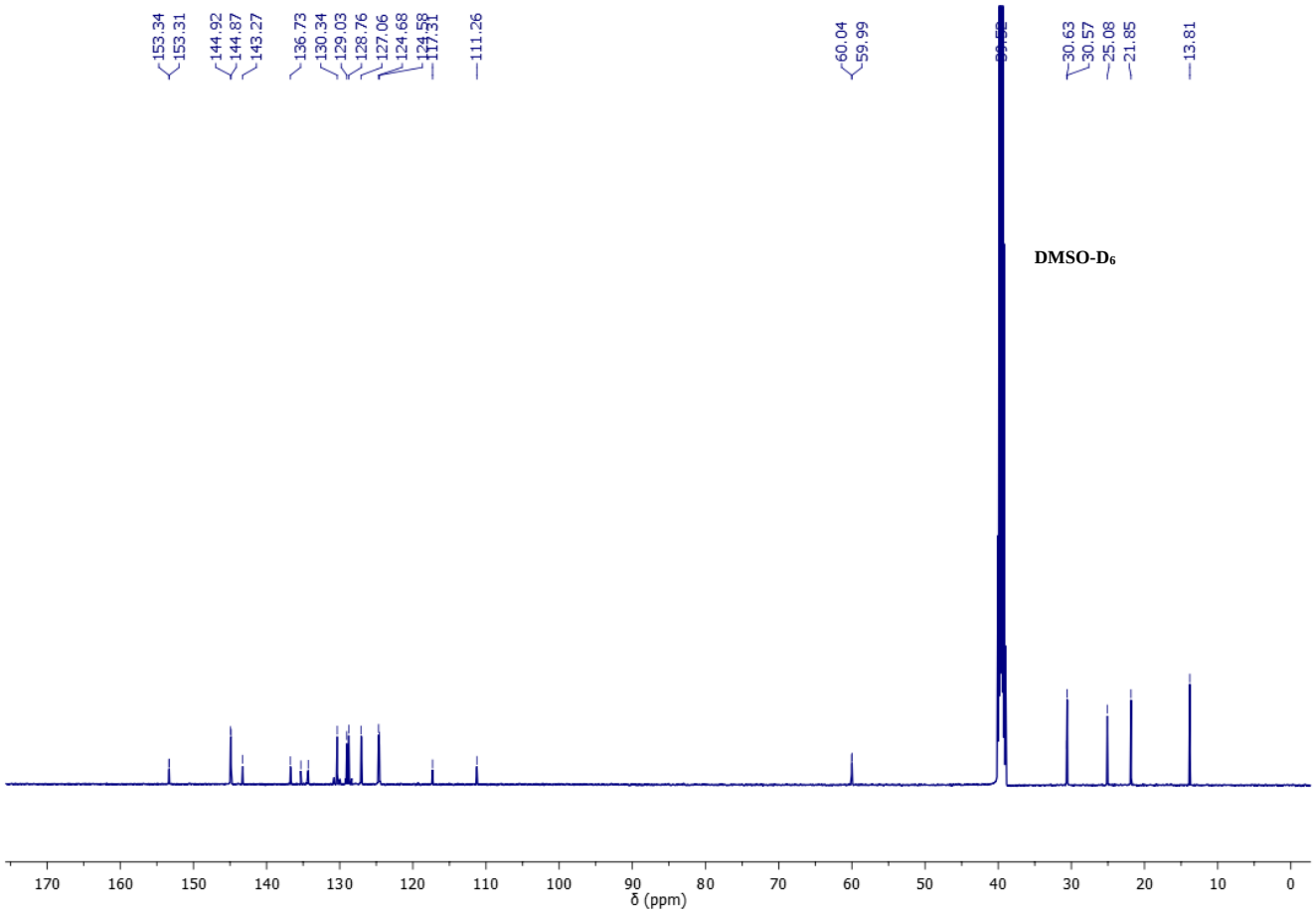

C. ESI Mass spectra of 6CS6:

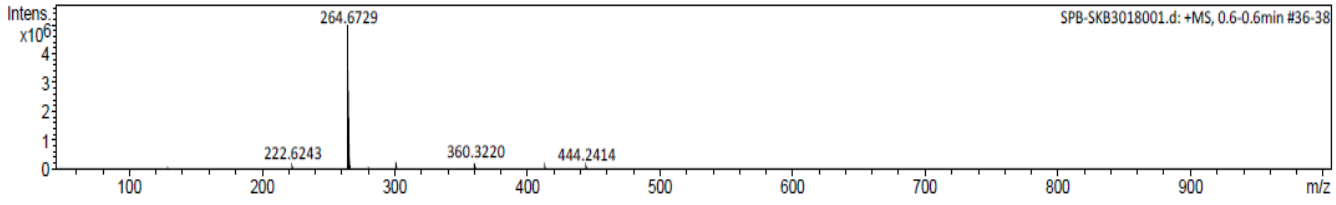

D. ^{1}H NMR spectra of 8CS8 (400 MHz, DMSO-D$_6$):

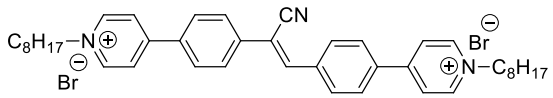

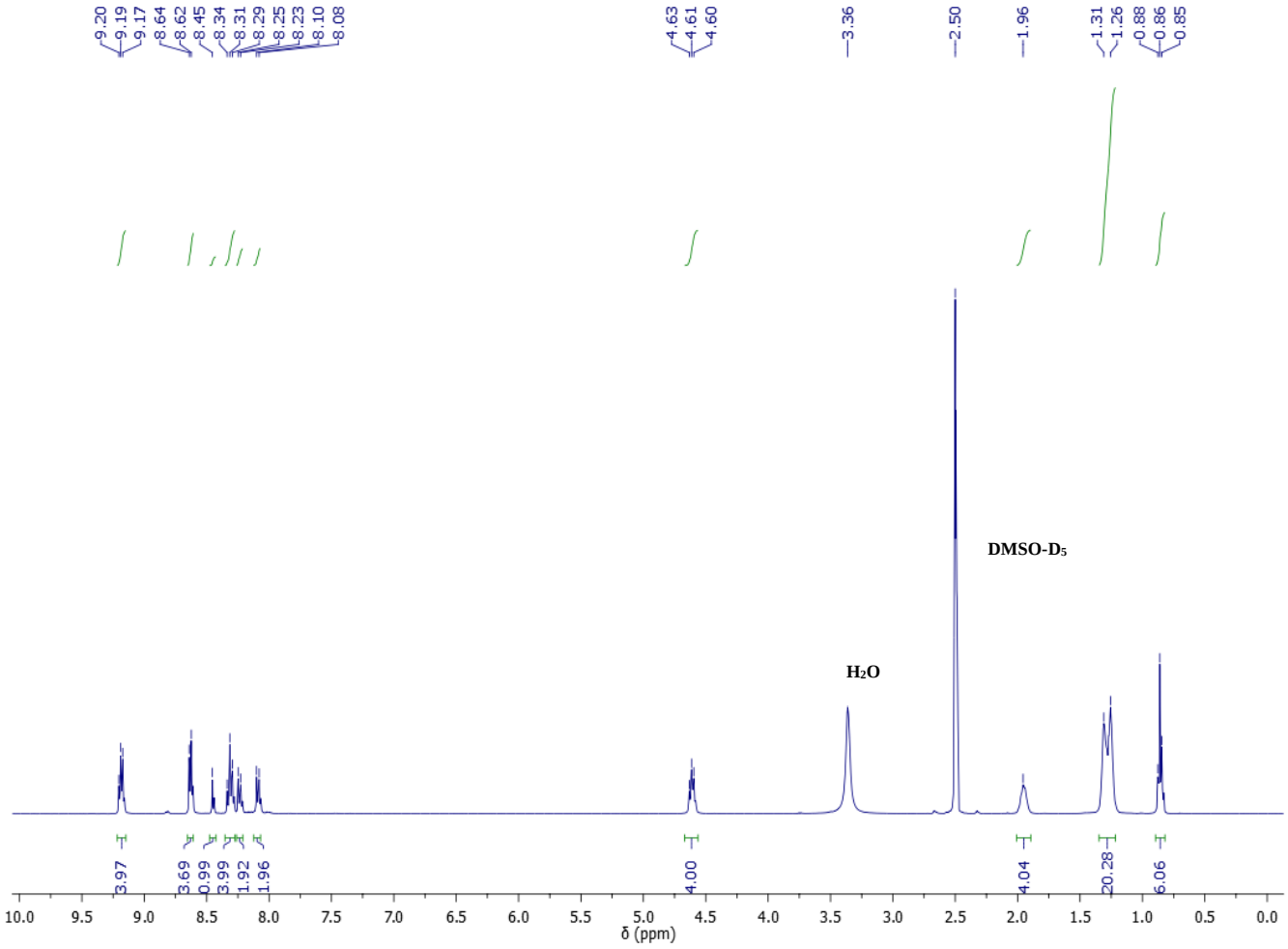

E. ^{13}C NMR spectra of 8CS8 (125 MHz, DMSO-D$_6$):

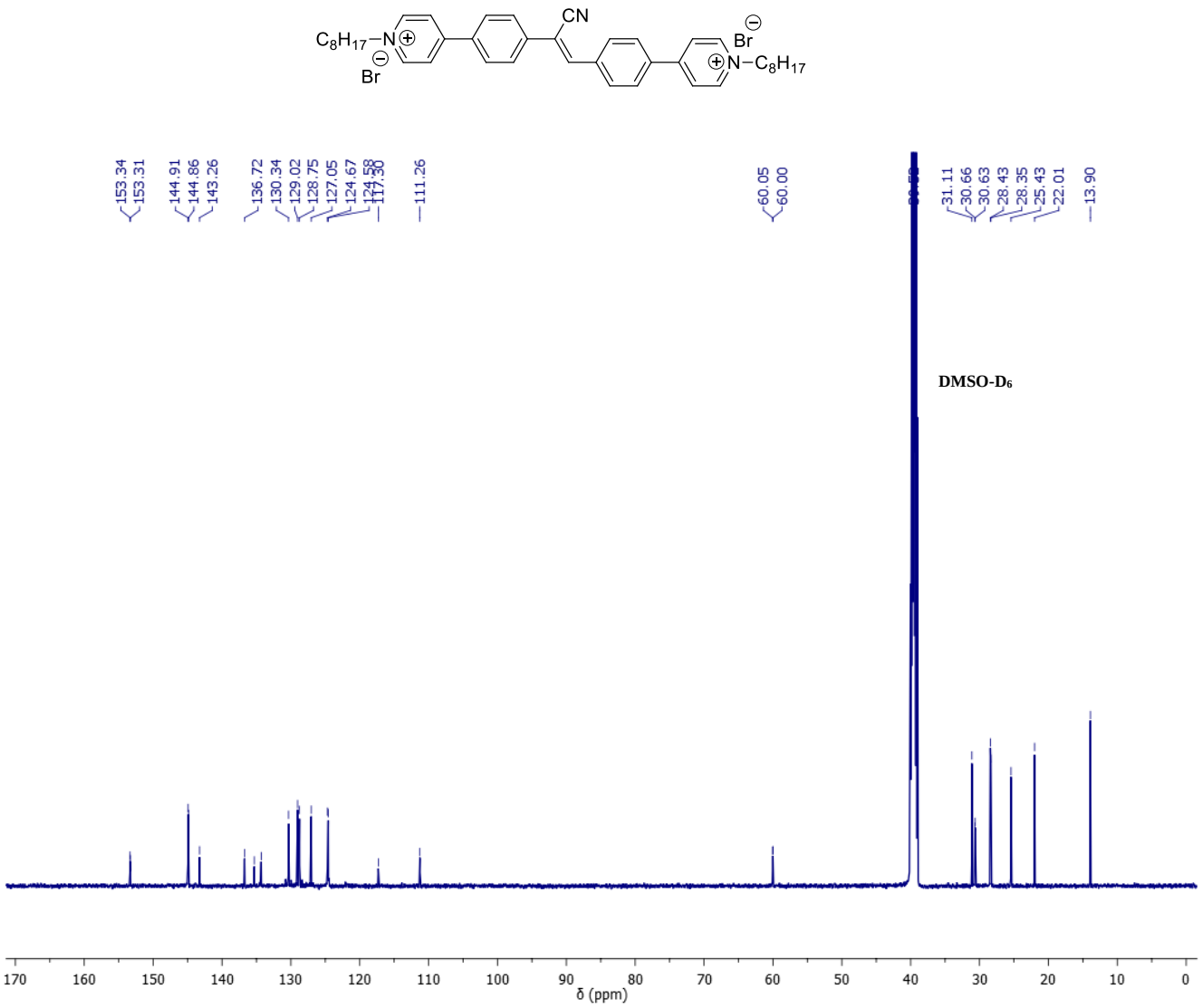

F. ESI Mass spectra of 8CS8:

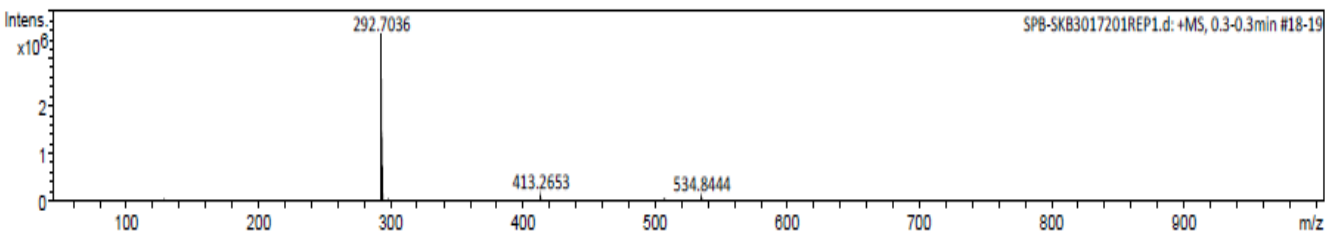

G. ^{1}H NMR spectra of 10CS10 (400 MHz, DMSO-D_6):

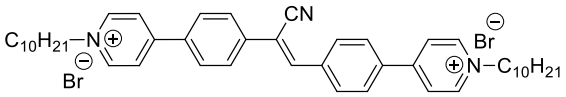

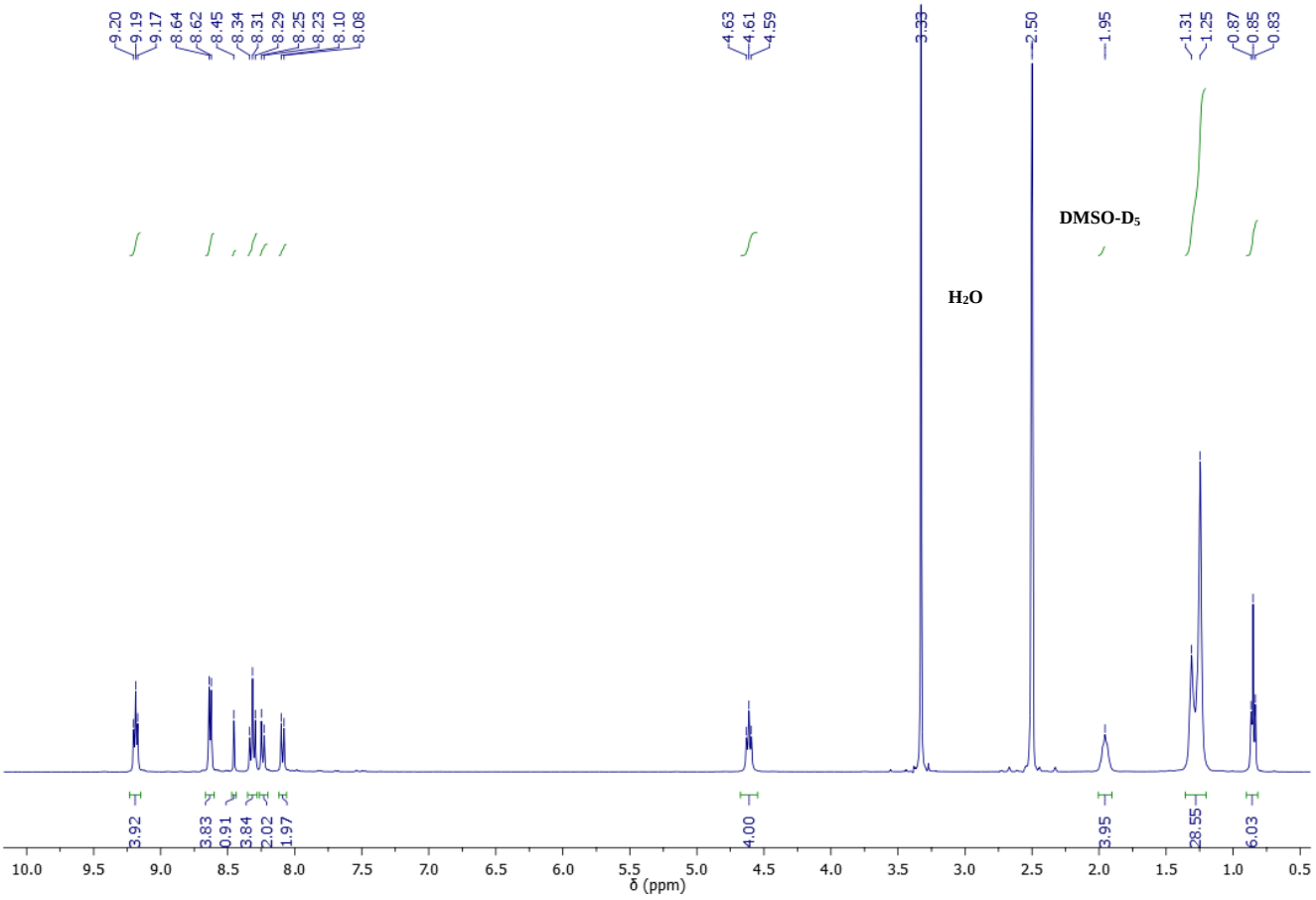

H. ^{13}C NMR spectra of 10CS10 (125 MHz, DMSO-D$_6$):

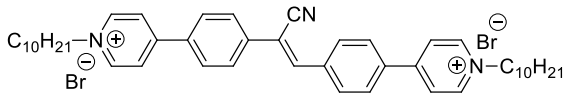

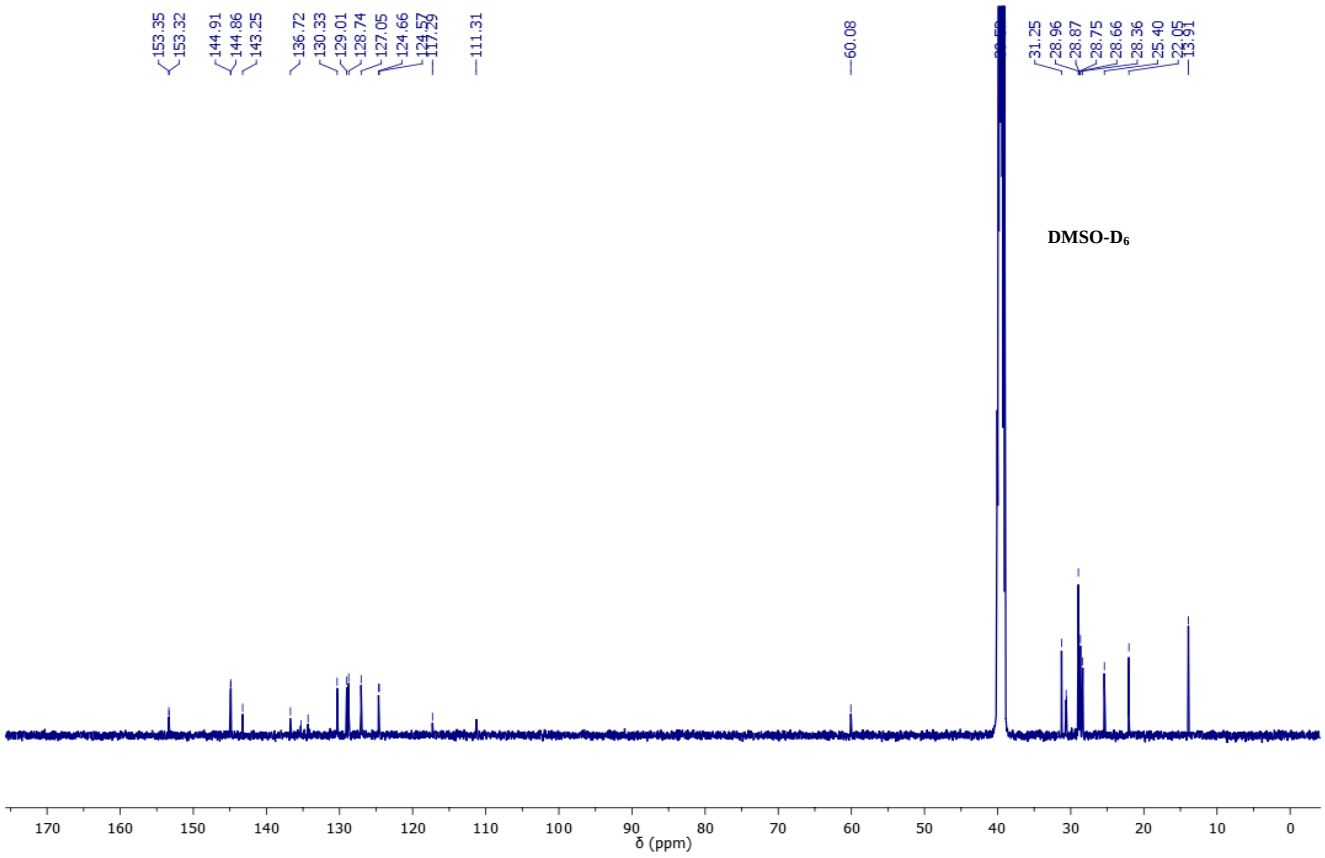

I. ESI Mass spectra of 10CS10:

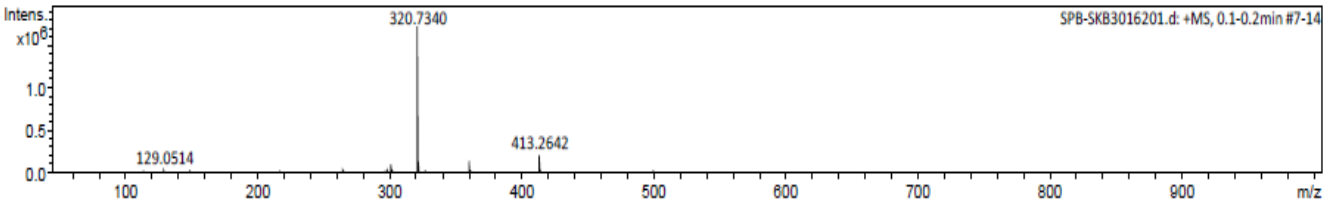

J. ^{1}H NMR spectra of 12CS12 (400 MHz, DMSO-D_6):

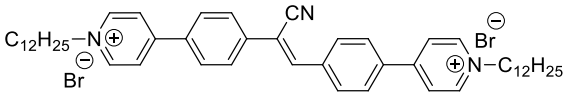

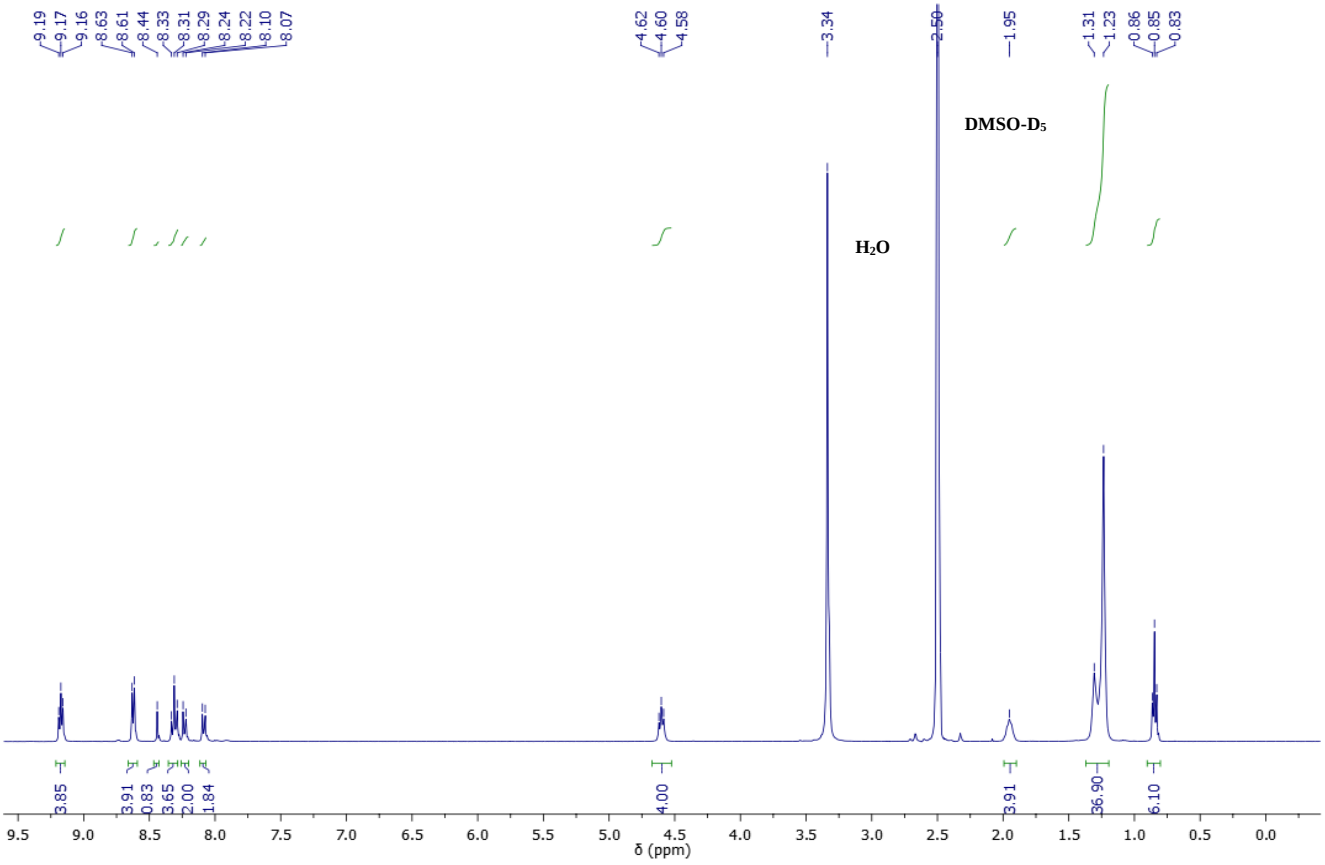

K. ^{13}C NMR spectra of 12CS12 (125 MHz, DMSO-D$_6$):

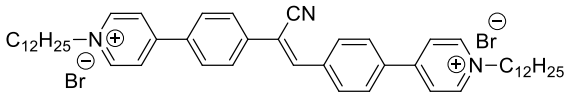

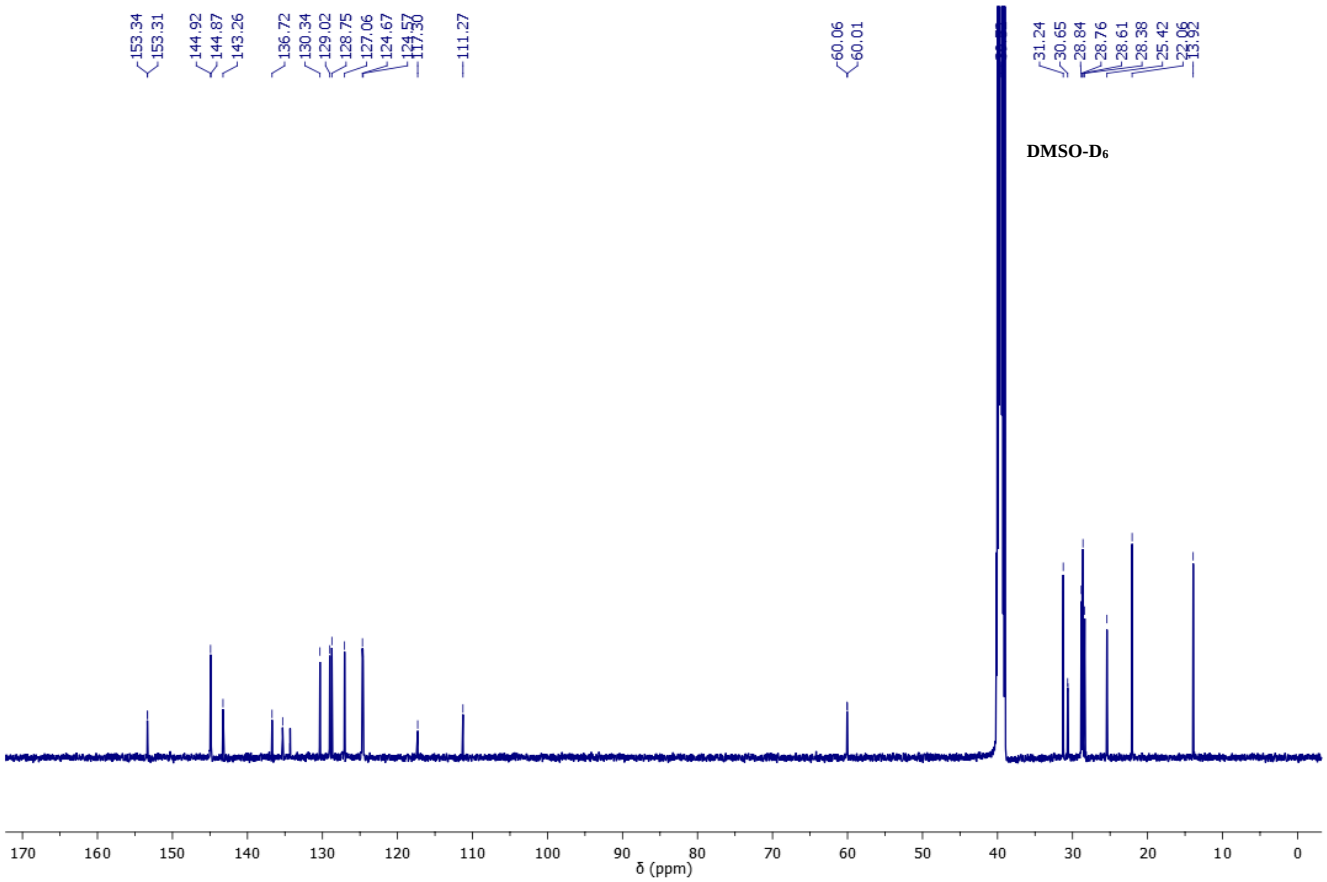

L. ESI Mass spectra of 12CS12:

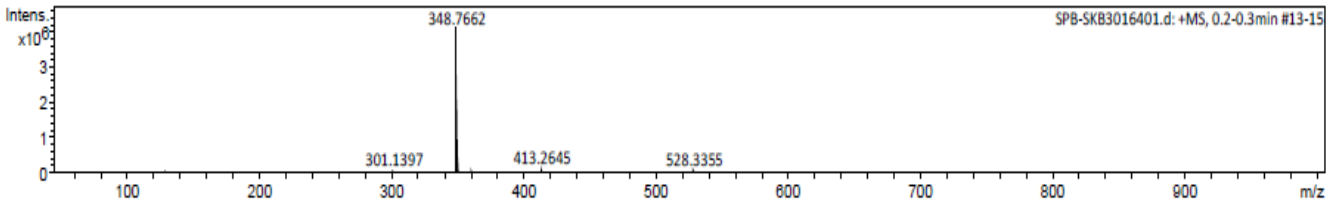

References

S1 M. J. Abraham, T. Murtola, R. Schulz, S. Páll, J. C. Smith, B. Hess and E. Lindahl, *SoftwareX*, 2015, **1–2**, 19–25.

S2 W. L. Jorgensen, J. Chandrasekhar, J. D. Madura, R. W. Impey and M. L. Klein, *J. Chem. Phys.*, 1983, **79**, 926−935.

S3 J. Huang and AD Jr. MacKerell, *J. Comput. Chem.*, 2013, **34**, 2135-2145.

S4 S. Jo, T. Kim, V. G. Iyer and W. Im, *J. Comput. Chem*., 2008, **29**, 1859-1865.

S5 K. Vanommeslaeghe, E. Hatcher, C. Acharya, S. Kundu, S. Zhong, J. Shim, E. Darian, O. Guvench, P. Lopes, I. Vorobyov and AD Jr. Mackerell, *J. Comput. Chem*., 2010, **31**, 671-690.

S6 B. Hess, H. Bekker, H. J. C. Berendsen and J. G. E. M. Fraaije, *J. Comput. Chem.*, 1997, **18**, 1463–1472.

S7 U. Essmann, L. Perera, M. L. Berkowitz, T. Darden, H. Lee and L. G. Pedersen, *J. Chem. Phys.*, 1995, **103**, 8577–8593.

S8 G. Bussi, D. Donadio and M. Parrinello, *J. Chem. Phys.*, 2007, **126**, 014101.

S9 M. Parrinello and A. Rahman, *J. Appl. Phys.*, 1981, **52**, 7182–7190.

S10 *(a)* S. K. Bhaumik, Y. S. Patra and S. Banerjee, *Chem. Commun.*, 2020, **56**, 9541—9544; *(b)* S. K. Bhaumik and S. Banerjee, *Analyst*, 2021, **146**, 2194–2202.

S11 H.-Q. Peng, Y.-Z. Chen, Y. Zhao, Q.-Z. Yang, L.-Z. Wu, C.-H. Tung, L.-P. Zhang and Q.-X. Tong, *Angew. Chem. Int. Ed.*, 2012, **51**, 2088–2092.